UNIVERSITY OF
KWAZULU-NATAL

INYUVESI
YAKWAZULU-NATALI

School of Engineering
Howard College Campus
Durban

Wetting and Separation Efficiency of Polypropylene Packing Modified by Nanoparticles

By:

Irshaan Sewlala

MSc Chemical Engineering
2018

Supervisor: Dr D Lokhat

(Examiners Copy)

A dissertation submitted to the School of Engineering
University of KwaZulu-Natal
Durban
In the fulfilment of the requirements of the degree of Master of Science in
Engineering

DECLARATION

The work presented in this dissertation was undertaken at the School of Engineering, University of KwaZulu-Natal, Howard College Campus in Durban, South Africa, from August 2017 until December 2018.

All work presented in this dissertation is original unless otherwise stated. It has neither in whole nor part been submitted previously to any other University or Institute as part of a degree.

I, Irshaan Sewlala, declare that

1.   The research reported in this thesis, except where otherwise indicated, is my original research.

2.   This thesis has not been submitted for any degree or examination at any other university.

3.   This thesis does not contain other persons' data, pictures, graphs or other information, unless specifically acknowledged as being sourced from other persons.

4.   This thesis does not contain other persons' writing, unless specifically acknowledged as being sourced from other researchers. Where other written sources have been quoted, then:
a.   Their words have been re-written, but the general information attributed to them has been referenced.
b.   Where their exact words have been used, then their writing has been placed in italics and inside quotation marks and referenced.

5.   This thesis does not contain text, graphics or tables copied and pasted from the Internet, unless specifically acknowledged, and the source being detailed in the thesis and in the References sections.

_____

Irshaan Sewlala

As the candidate's supervisor(s)/co-supervisor I hereby certify that I find this work to be suitable for submission for the degree of Master of Science in Chemical Engineering.

_____

Dr. David Lokhat
(Supervisor)

ACKNOWLEDGEMENTS

I would like to take this opportunity to acknowledge and show my deepest gratitude to the following people who have all greatly contributed to the completion of this dissertation:

- First and foremost, I would like to thank my parents, my brother, my friends and family, for giving me the strength, motivation and support to pursue my MSc degree and other endeavors in life.

- My supervisor, Doctor David Lokhat, for imparting on me his vast knowledge, invaluable expertise, constructive critique and guidance for the entirety of the project.

- The lab technicians: Ms. Xoli Hadebe and Ms. Thobekile Mofokeng as well as the chemical engineering technical staff: Mr. Danny Singh, Mr. Sanjay Deeraj and Mr. Gerald Addieah. Thank you for your valuable assistance throughout my work.

- Final year chemical engineering students of 2017: Ms. Janine Alessandra Govender and Ms. Shazelle Vinette Govender, for their valued assistance with experimental runs during their laboratory work module.

- Final year vacation work students of 2018: Mr. Ishaaq Lakhi, Mr. Mehul Shah and Ms. Kashmita Ramlal, for their valued assistance with experimental related work during their vacation work module.

EXECUTIVE SUMMARY

Packed columns are one of the main unit operations used in distillation, extraction, absorption and hydrotreating due to their ease of operation, versatility and adaptability to different chemical systems. The distribution of gas and liquid over the packing material is the basis of separation. Selection of the type of packing material is a crucial step in column design as the separation efficiency of the column is dependent on the ratio of wetted area to the total available surface of packing, known as the wetting efficiency. Glass and metal packing offer superior wetting efficiency when compared to random packing fabricated from plastic. Plastic packings offer better chemical resistance in selected systems, as well as being more lightweight and cost-effective. Literature indicates that the wetting behaviour of glass, metal and polymeric substrates may be modified by applying multilayer coatings of nanoparticles. These nanoparticles are often silica based. In this work, polypropylene random packing was modified by first being treated with the Piranha solution and then being coated by silica nanoparticles that were produced via the Stober Process. The first part of this project investigates the employment of a stimulus response technique in which an inert salt tracer is injected into an inlet liquid stream, pumped by a peristaltic pump, and allowed to flow over the packing material. The packing material being investigated in this study are glass, unmodified and modified polypropylene Raschig rings. The residence time distribution, reported as the mean residence time (MRT), and exit age distribution were determined for the three types of packing used in this study. By comparison to standard distribution curves obtained from the literature, the experimental exit age distribution curves were used to estimate the wetting efficiency of the different packing. The glass and unmodified packing had a MRT of 12 seconds while the modified packing was 19 seconds. The wetting efficiencies were 0.3, 0.4 and 0.8 respectively. The increase in MRT indicates that fluid elements resided in the column packed with modified polypropylene for a longer period while the increase in wetting efficiency shows clear improvement in wettability for the modified packing. For the second part of the study the absorption performance of the different packings was investigated. A system of water and carbon dioxide was selected to be used in the study as it is a very simple, non-toxic system and performance can be analysed using the titration method. For the 280 mm and 90 mm packed height with a 16 % carbon dioxide inlet concentration, modified packing showed improvements on absorption for all liquid flowrates for up to 10.24 % and 9.36% respectively when compared to the unmodified packing. The silica nanoparticle modification to the polypropylene packing was successful as overall, it performed better than the unmodified packing in absorption performance

TABLE OF CONTENTS

LIST OF FIGURES

Appendix C

LIST OF TABLES

Appendix C

NOMENCLATURE

Symbol	Description	Units
C	Concentration	g/ml
E(t)	Exit Age Distribution	s
M	Mass	g
t	Time	s
Δt	Time Interval	s
Q	Volumetric Flowrate	$ml/s = cm^3/s$
Greek Symbols		
τ	Mean Residence Time	s
Abbreviations		
DV	Dead Volume	cm^3
MRT	Mean Residence Time	s
PP	Polypropylene	-
RTD	Residence Time Distribution	s
SEM	Scanning Electron Microscope	-
ST	Space Time	s

CHAPTER 1: INTRODUCTION

Distillation involves the thermal separation of chemical components within a column filled with trays or packed to a specific height with random or structured packing. The uniform distribution of fluids and the formation of a thin liquid film over the surface of the packing elements is the basis of separation. In practice two closed fluid phases move counter currently whilst mass transfer occurs. The efficiency of the packing inside the column for a separation, i.e. the effective height of an equilibrium stage, is related in part to the wetting behaviour of the packing material.

The wetting of a solid surface with a liquid is critically important to process unit operations such as distillation, absorption and stripping. The ratio of effective surface area of material (i.e. covered by liquid) to the total available surface area is referred to as the degree of wetting. The degree of wetting in packed columns is important since it is this parameter that determines the total effective interfacial area for mass transfer in the unit (Krell, 1982). Random packings fabricated from plastic offer distinct advantages in certain cases over ceramic or metal packings, viz. better chemical resistance in selected systems, lightweight, cost-effective (Krell, 1982). In aqueous systems, the degree of wetting on plastic components can be poor, which results in relatively poor performance of the separation unit. The wetting of the solid surface in a separation unit is a complex phenomenon which depends on many factors (Ataki, 2006): liquid properties such as viscosity; density and temperature; solid-liquid interaction; shape and size of packing; operating conditions inside the column, e.g. liquid load in a packed column.

There has been a large body of work published on the design of packed separation units (Sieder and Henley, 1998). Most design studies have focused on optimization of liquid distribution in the column or the packing structure. In only a few cases have researchers looked at modification of the surface characteristics of the packing. Ponter et al. (1976) investigated the effect of adding an interface-activating substance to the liquid on the efficiency of a packed column. They observed an increase in the separation efficiency corresponding to a change of the wetting behaviour as determined by contact angle measurements. The degree of wetting of packings, and consequently the separating efficiency depends on the average degree of roughness of the material (Krell, 1982). It also depends on the physicochemical interaction between the liquid and the solid surface. In recent years, it has been shown that the wetting behaviour of glass, metal and polymeric substrates can be modified by applying multilayer coatings of nanoparticles (Athauda et al., 2012; Hwang and Ahn, 2015). These

nanoparticles are often silica based. By modifying the surface characteristics of the plastic packing, the degree of wetting and hence separation efficiency can be improved. These modified materials exhibit very low contact angles and hence vastly improved wetting behaviour. These materials have never been tested as a packing in a vapour-liquid separation system, in which they have the potential to improve the wetting and separation efficiency.

In a packed column, a stimulus response technique can be used to experimentally measure the residence time distribution of the liquid phase. Usually an inert tracer is injected into the liquid inlet stream and the concentration of the tracer in the exit stream is measured as a function of time. Construction of the exit age distribution curve from experimental data and comparison to the distribution curves given in the work of Julcour-Lebigie et al (2007) allows for the determination of the wetting efficiency of the column. The location of the peak in the distribution curve can be correlated against the wetting efficiency of the packing. In packed columns, mass transfer efficiency is related to the intimate contact between the liquid and vapour phases. The most commonly used parameter that relates the height of a packed column and the separation efficiency is the HETP or Height Equivalent to Theoretical Plate. This concept is useful in comparing the separation efficiency of different packings for a system.

This study has been broken up into two parts. Part A involves the modification of the polypropylene Raschig rings and the determination of its wetting efficiency. One means of altering the wettability of polymeric materials is to pre-treat the polypropylene packing with a piranha solution followed by depositing the silica nanoparticles, produced via the Stober Process, on the surface to produce the modified polypropylene Raschig rings. The modified polypropylene Raschig rings were compared to unmodified polypropylene and glass Raschig rings in this study. Construction of the exit age distribution curve from experimental data and comparison to standard distribution curves given in the work of Julcour-Lebigue et al (2007) allowed for the estimation of the wetting efficiency for the three types of Raschig rings previously mentioned. SEM/EDX analysis were undertaken on the modified and unmodified Raschig rings to confirm that the silica nanoparticles attached onto the polypropylene Raschig rings. Part B of the study involved experiments to determine the absorption performance of the modified packing. The experiments were performed in a glass columns packed with the three previously mentioned Raschig rings to a specific height. Carbon dioxide and water was the system chosen to perform these tests on as it is a simple, non-toxic system while the performance could be measured using a titration performed with sodium hydroxide and hydrochloric acid. Varying inlet concentrations of carbon dioxide as well as L/G ratios in the column and packed height, absorption performance of the different Raschig rings could be compared.

This research project aims to answer the following research questions:

1. Can the wetting efficiency of random packings fabricated from polypropylene be improved by coating with silica nanoparticles?

2. Is the overall separation efficiency of a packed column improved with the use of these modified random packing materials, and if so what is the quantitative change in the separation efficiency?

3. How does the modification of the degree of wetting of the packing material qualitatively affect the hydrodynamic characteristics of the liquid in the column?

The objectives of this research project are:

1. To produce standard polypropylene Raschig rings, pre-treat it with the piranha solution and thereafter coat with silica nanoparticles.

2. To determine the residence time distribution, exit age distribution and estimate the wetting efficiency using standard curves obtained from literature for each type of Raschig rings.

3. To investigate if the modification of the polypropylene Raschig rings with a silica nanoparticle coating improved the wetting efficiency and absorption performance of the packing.

4. To investigate the effects of L/G ratios, packed height and inlet concentration of carbon dioxide on the absorption performance of the different Raschig rings.

Outline of the Dissertation

This dissertation was divided into four parts:

1. The theoretical background of this research topic: covered in Chapter 2.

2. The experimental methods undertaken for this study: covered in Chapter 3.

3. A discussion of results obtained throughout this study: covered in Chapter 4.

4. The conclusions formed at the completion of the study: covered in Chapter 5.

With the aid of the results presented in this dissertation, the development, wetting efficiency and absorption performance of the modified polypropylene Raschig rings may be analysed.

CHAPTER 2: LITERATURE REVIEW

2.1 Gas-liquid mass contactors

Gas-liquid mass contactors are types chemical equipment used for mass transfer between a gas phase and a liquid phase. Gas-liquid mass contactors are divided into two main categories known as differential gas-liquid contactors and stage wise gas-liquid contactors. Differential gas-liquid contactors include packed columns, spray towers and bubble columns. Mass transfer occurs within the entire length of the column. Stage wise gas-liquid contactors include plate columns and venture tubes. Mass transfer occurs within each stage of the columns as vapor-liquid equilibrium is reached.

2.1.1 Main Unit Operations

<u>Absorbers</u>

Absorbers are columns that bring gas and liquid phases in contact, so that impurities or desired products in the gas phase absorb into the liquid phase because of their interaction. The species transferred to the liquid phase are referred to as solutes. Absorption involves no change in the chemical species present in the system. The liquid stream enters at the top of the column and exits at the bottom while the gas enters at the bottom of the column and exits at the top. Absorbers are used in the chemical, petrochemical and the water treatment industry mainly for environmental regulations on gaseous emissions.

<u>Strippers</u>

 Strippers are columns that bring liquid and gas phases in contact, to remove impurities or desired product from the liquid phase into the gas phase due to their interactions. Stripping is the inverse of absorption liquid mixture are separated by contacting the feed with a vapour stripping agent (Seader & Henley, 2006). The species transferred to the gas phase are referred to as solutes. The liquid stream enters at the top of the column and exits at the bottom while the gas enters at the bottom of the column and exits at the top. Strippers are generally used in industry for the removal of harmful contaminants from waste streams.

<u>Distillation Columns</u>

Distillation columns involve a liquid or gas mixture of two or more species being separated into its component fractions of desired purity by the application and removal of heat. It is based on the

principle that the vapour of the boiling mixture will be richer in the species that have the lower boiling points. One or more inlet streams are sent into the column at a specific temperature and pressure with the column have two or more exits streams. The two essential exit streams are located at the top and bottom of the column. The exit stream at the top is a vapour stream while the liquid stream exits at the bottom. Side exit streams may also appear in a column between the top and bottom exits to extract another desired product. The liquid within the column will move down while the gas moves up while in contact with trays or packing material in the column. Reboiler and condensers are connected to the exit liquid and gas streams respectively to provide a reflux back into the column. The operating pressure and temperatures and feed location are important variables to consider when designing a distillation column. Distillation columns are widely used in the chemical process industries such as petroleum processing and production, natural gas processing, coal tar processing and brewing.

2.1.2 Calculation Approach

Mass and Energy Balances

The law of conservation of mass states that "mass in an isolated system is neither created nor destroyed by chemical reactions or physical transformation (Smith & Van Ness, 2005)." A mass balance on a column follows the same principle meaning, the total mass entering the column will equal to the total mass exiting the column as no consumption and generation occurs in the column. This principle stays true for total mass and mass of specific species for the column. These calculations are vital for column design and determining its performance. Figure 2.1 below shows a simple diagram of an absorber.

$L_t, x_{A,t}$ $V_t, y_{A,t}$

$L_b, x_{A,b}$ $V_b, y_{A,b}$
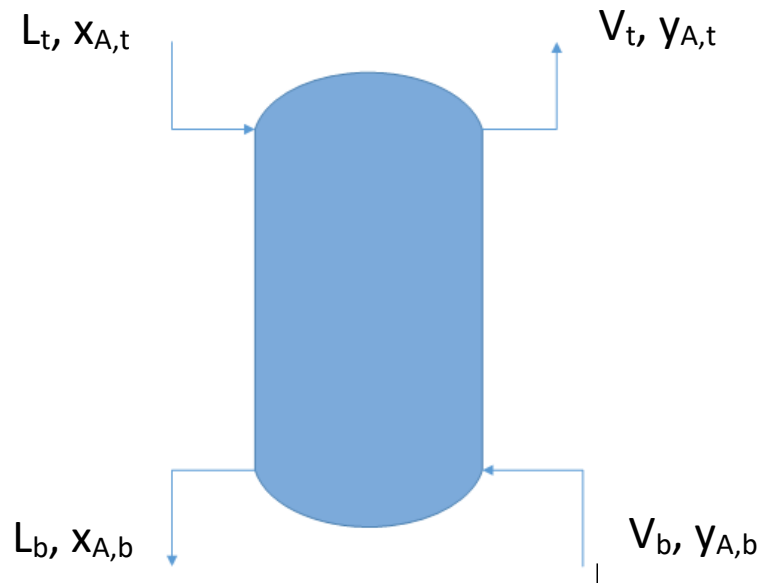
Figure 2.1: Diagram of an absorber column

The following mass balance equations can be used to determine unknown values for an absorber.

$$L_t + V_b = L_b + V_t \tag{2.1}$$

Where   V = vapour flowrate

                   L = liquid flowrate

                   t, b = top and bottom of tower, respectively

$$L_b x_{Ab} + V_t y_{A,t} = L_t x_{A,t} + V_b y_{A,b} \tag{2.2}$$

Where y_A = mole fraction of A in the vapour phase

                   x_A = mole fraction of A in the liquid phase

Equation 2.1 represents the overall mass balance for the absorber while equation 2.2 is a mass balance for the species A. The same principles are used for mass balances conducted on strippers and distillation columns.

Energy balances follows the first law of thermodynamics which state which states that, "the change in internal energy of a system equals the net heat transfer into the system plus the work done on the system." The general energy balance equation can be seen below in equation 2.3.

$$\dot{Q} - \dot{W} = \sum_{out}(\dot{m}\,\Delta H) - \sum_{in}(\dot{m}\,\Delta H) \tag{2.3}$$

Where $\dot{Q}$ = heat transferred

$\dot{W}$ = work

$\dot{m}$ = mass flowrate of a species

ΔH = Change in enthalpy of a species

In an absorber, stripper and distillation column, no work is done on the system therefore the work term on the equation can be omitted. The mass flowrates of the species in a stream can be determine by multiplying the total mass flowrate of the stream by the mole fraction of that species in the stream while the enthalpy values. If the $\dot{Q}$ value is positive heat has been absorbed by the system while when negative heat has flowed out of the system.

Graphical techniques to determine column performance

The graphical method to evaluate minimum number of stages, theoretical number of stages and compositions of inlet and outlet streams is known as the MaCabe-Thiele method. To procedure with this method an equilibrium curve and operating line needs to be obtained. The equilibrium curve can be plotted with equilibrium data obtained from literature for the system. In the case of absorption and stripping, the equilibrium curve is usually a straight-line due it being a dilute solution. The operating line for an absorber can be obtained using equation 2.4 below. For dilute mixture, the liquid and vapour flowrates maybe be assumed to be constant throughout the column.

$$y = \frac{L}{V}x + \frac{y_1 V_1 - x_0 L_0}{V}$$
(2.4)

Where L = liquid flowrate

V = vapour flowrate

y_1 = vapour mole fraction of the solute exiting the column

x_0 = liquid mole fraction of the solute entering the column

Once both lines are obtained, the stepping of the stages can be done. For absorption, the stepping starts on the operating line at the coordinates (x_0, y_1). A horizontal line is then drawn to the equilibrium curve and is followed by a vertical line being drawn back to the operating line. This process is repeated for the required number of stages or until the step intercepts the coordinates (x_N, y_{N+1}).

For a distillation column, the operating line is split into two parts, the stripping and rectifying section. The operating line for the stripping section is obtained by drawing a straight line from the coordinates of the composition of the feed, (x_F, y_F), to the coordinates of the bottoms product, (x_b, y_b). The operating line for the rectifying section is obtained by drawing a straight line from the coordinates of the composition of the feed, (x_F, y_F), to the coordinates of the tops product, (x_t, y_t).

 Numerical techniques to determine column performance

The Kremser equation is a numerical method to calculate absorption or stripping factor within a absorber or stripper. To use the Kremser equation the liquid and gas mixtures must dilute and the equilibrium curve must be a straight line. Equation 2.5 below shows the Kremser equation for an absorber.

$$\frac{y_{N+1} - y_1}{y_{N+1} - y_0^*} = \frac{A^{N+1} - A}{A^{N+1} - 1} \tag{2.5}$$

Where   A = absorption factor

               y = liquid mole fraction of solute

The same equation may be used for a stripper by replacing the absorption factor (A) with a stripping factor (S).

2.1.3 Packed and Trayed Columns

Packed Columns

A packed column is a vertical, cylindrical pressure vessel containing one or more sections of a packing material. Liquid flows downward by gravity over the packing, as a film or as droplets between packing elements (Seader & Henley, 2006). Packed columns are extensively used in industry including the chemical, petrochemical or even water treatment industry. A variety of unit operations are commonly carried out in packed columns such as absorption, extraction and distillation. The gas liquid contact in a packed bed column is continuous, not stage-wise, as in a trayed column. In most cases liquid enters the vessel and falls over the packing by gravity whilst gas enters counter-currently or co-currently and contacts with the falling liquid. Thus, mass transfer occurs between phases. The performance of a packed column is mainly dependent on the maintenance of good liquid and gas distribution throughout the column.

A typical packed column arrangement consists of a tubular metal or glass vessel with liquid and gas inlets and outlets. The liquid inlet is most commonly found at the top of the column as the liquid flows over the packing by gravity. A liquid distributor is also commonly found and is used to distribute the flowing liquid as uniformly as possible over the entire cross sectional area of the column as it enters the packing section. The packing elements that make up the fixed bed are supported in the column by support grids that prevent the separation and random movement within the column. Figure 2.2 shows a typical industrial packed column.
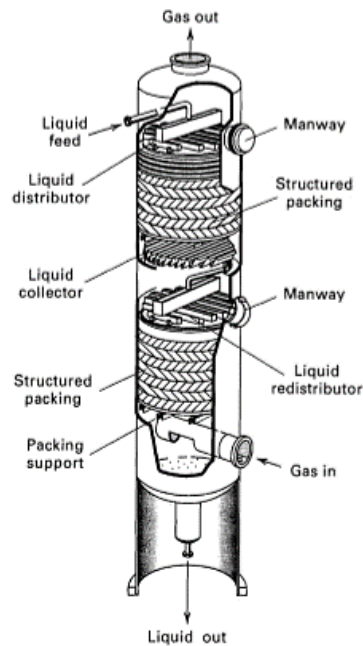
Figure 2.2: Schematic of a packed column (Seader & Henley, 2006).

Trayed Columns

A trayed tower is a vertical, cylindrical pressure vessel in which vapor and liquid, flowing counter currently, are contacted on trays or plates that provide intimate contact of liquid with vapor to promote rapid mass transfer (Seader & Henley, 2006). Liquid flows across each tray, over an outlet weir, and into a downcomer, which takes the liquid by gravity to the tray below. Gas flows upward through openings in each tray, bubbling through the liquid on the tray (Seader & Henley, 2006). For ideal cases, the vapour in the column carries no liquid droplets, which is known as entrainment, to the above trays while the liquid in the column carries no vapour bubbles, which is known as occlusion, to the tray below. There showed also be no weeping of the liquid through the holes in the tray (Seader & Henley, 2006).
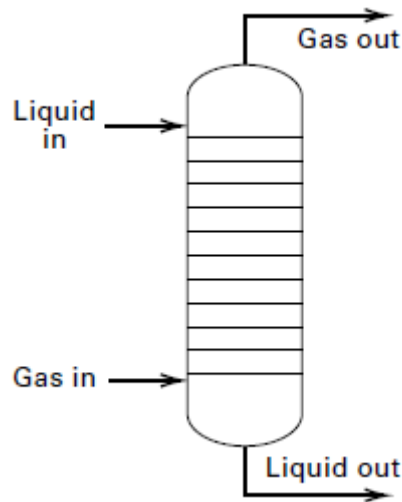
Figure 2.3: A diagram of a trayed column (Seader & Henley, 2006)

Equilibrium between the exiting vapour and liquid phases is approached on each tray (Seader & Henley, 2006). The three main types of trays used are sieve trays, valve trays and bubble-cap trays. Sieve or perforated trays have perforations, usually one eighth to half an inch in diameter, as tray openings for the vapour to pass through. Valve trays have openings, usually from one to two inches in diameter, containing a valve consisting of a cap that overlaps the hole (Seader & Henley, 2006). Without vapour flow the valves will be closed and as the vapour rate increases the valve rises, creating a bigger opening. Bubble-cap trays consists of a cap around three to six inches in diameter. The cap has triangular or rectangular slots cut around its side (Seader & Henley, 2006) which allows the vapour to flow through it. In Table 2.1 below, the different types of trays are compared.

Table 2.1: Comparison of types of trays (Seader & Henley, 2006)

	Sieve Trays	Valve Trays	Bubble-Cap Trays
Relative cost	1.0	1.2	2.0
Pressure drop	Lowest	Intermediate	Highest
Efficiency	Lowest	Highest	Highest
Vapor capacity	Highest	Highest	Lowest
Typical turndown ratio	2	4	5

2.1.4 Types of Packing

Packing section in the absorption process plays important role providing surface area for the gas and liquid phases to contact upon (Arachchige & Melaaen, 2012). Packing material should be chemically inert to fluids, strong enough without excessive weight, provide good contact between liquid and gas, be reasonable in cost and provide adequate passage without excessive hold up or pressure drop (Saeed et al, 2015). Glass and metal packing are commonly used due to their superior wetting efficiency, however, random packing fabricated from plastic offer distinct advantages in certain cases for better chemical resistance in selected systems, lightweight and cost-effectiveness (Krell, 1982).

Structured Packing

Structured packing may be found in the form of corrugated metal gauze or plastic sheets. The uniform arrangement of structured packing provides some advantages when compared to random packed or trayed columns. These advantages include, lowering the pressure drop through the column, increasing efficiency in the same height tower as well reducing the vessel diameter to obtain the same separation. Structed packing is designed to increase the contact time of the liquid and gas by forcing them to take complicated paths within the column. Metal gauze is the preferred for low liquid rate and deep vacuum applications while plastic sheets can handle a wider range of liquid and flow rates and offer better chemical resistance in selected systems. Structured packings tend to offer higher efficiency and capacity, as well as lower pressure drop than random packings.

Random Packing

Random or dumped packing is made up of small individual elements such as Raschig rings, Berl saddles or Pall rings that are poured into the column and orient themselves randomly (Figure 2.4). Raschig rings are small hollow cylinder having a length about equal to the diameter. Metal and plastic rings are more efficient than ceramic rings, as it is possible to make the walls thinner.
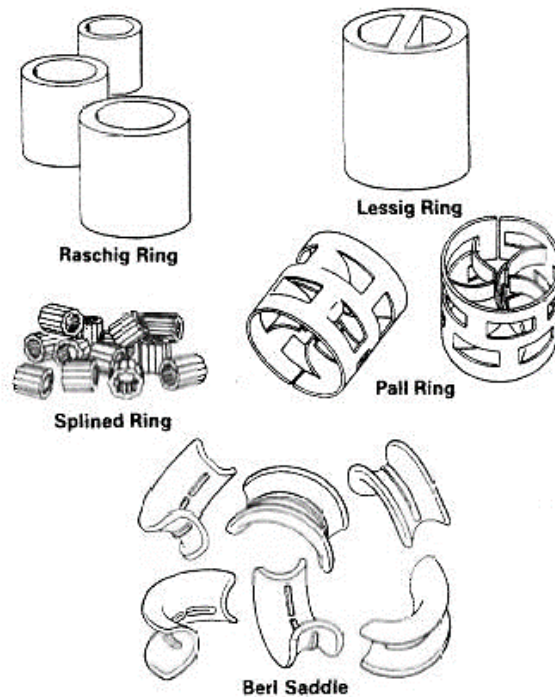
Figure 2.4: Types of random packing (Seader & Henley, 2006).

The major benefit of random packing is that it is more cost effective than structure packing and less sensitive to misdistribution. Pall rings are most preferred and commonly use random packing but their cost per unit volume is high. Pall Rings required minimum diameter and minimum height for the given absorption or distillation duty as compared to other types of the random packings. Pall rings are available in metal and plastics (Ataki, 2006). Pall rings are available at a size of 50 mm in ceramic, metal and plastic while only in metal and plastic for 15, 25 and 35 mm sizes. Berl saddle packing performs better as compared to Raschig rings in the aspects of even fluid distribution and low resistance while also lowering the pressure against the inner walls of the column. Berl saddles are ceramic and are available at a size of 13 and 25 mm. Raschig rings can be in the form of ceramic, metal and plastic at a wide range of sizes due to its simple and cost-effective design.

2.2 Measurement of wetting efficiency of packing in a packed column

2.2.1 Residence Time Distribution (RTD)

The residence time distribution refers to a probability distribution that describes the amount of time individual fluid elements spend in a vessel. Different elements of the fluid spend different amounts of time within the vessel and thus the overall performance of a reactor is dependent on the residence time distribution

A stimulus response technique can be used to experimentally measure the residence time distribution. An inert salt tracer is injected into the liquid inlet stream and the concentration of the tracer in the exit stream is inferred as a function of electrical conductivity and time. The selected tracer should be non-reactive and should not change the hydrodynamics of the system. The tracer should also be easily detectable. Using this technique, the wetting efficiency can be determined while the bed is under operation. The packed column was assumed to operate with steady flow, plug flow with axial dispersion and negligible tracer vaporization (Julcour-Lebigue et al, 2007).

The stimulus response technique utilizes two different input methods. These are the pulse input method and the step input method. Each gives rise to a different response after the tracer has been injected. A pulse input is favoured as the method of injection because it provides information on the distribution of residence times. In a pulse input, the tracer is suddenly injected into the system as fast as possible. The exit concentration is inferred producing a pulse response as seen in figure 2.5 below.
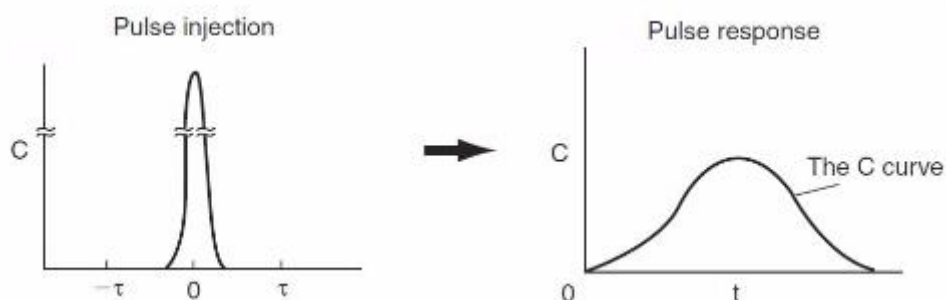
Figure 2.5: Pulse Injection and the Resulting Pulse Response (Fogler, 1999).

This brings about a distribution of times of fluid elements leaving the column, known as the exit age distribution. The exit age distribution is calculated as follows:

$$E(t) = \frac{Ci}{Area} \qquad (2.6)$$

Where the area of the curve is calculated using the following summation:

$$Area = \sum Ci\Delta t \qquad (2.7)$$

Considering the assumptions of axial dispersion and constant volumetric flowrate through the column, the space time of the reactor and mean residence time are taken to be equal. The mean residence time can then be defined as the average time taken for fluid elements to pass through the packed column. The mean residence time, τ, can then be calculated as follows based on discrete concentration-time points:

$$\tau = \frac{\sum Ci \cdot ti \cdot \Delta t}{\sum Ci\Delta t} \qquad (2.7)$$

Where:

τ = Mean residence time (s)

C_i = Concentration (ml saturated salt solution/ml water)

t_i = time (s)

Δt = time interval (s).

2.2.2 Wetting efficiency

Process unit operations such as distillation, absorption and stripping are largely dependent on the wetting of a solid surface with a liquid. The degree of wetting is given by the ratio of effective surface area of material (i.e. covered by liquid) to the total available surface area. The degree of wetting in packed columns is important since it is this parameter that determines the total effective interfacial area for mass transfer in the unit (Krell, 1982). The wetting of the solid surface in a separation unit is a complex phenomenon which depends on a variety of factors such as liquid properties including; viscosity, density and temperature (Ataki, 2006). Solid – liquid interaction parameters as well as the

operating conditions of the packed column are also important, not to forget the physical and chemical characteristics of the packing being used within the column. To obtain a high wetting efficiency (f > 0.3), the liquid should thoroughly wet the surface of the packing material. The performance of the packed tower is directly proportional to the wetting of the entire packed area.

Wetting efficiency is estimated by comparing the experimental exit age distribution curve with standard curves obtained from Julcour-Lebigue et al (2007) which correlate exit age distribution to wetting efficiency. The shape and position of the resulting second peak and tail of the experimental exit age distribution curve can be compared to that of standard distribution curves shown in Figure 2.6 below to estimate the wetting efficiency, f. The initial signal peak represents the bulk liquid leaving the column and is therefore not useful in estimating the wetting efficiency. The second peak and tail represent the interstitial liquid that remains in the column adhering to the packing material and side walls for a period of time which is considered to be the mean residence time.
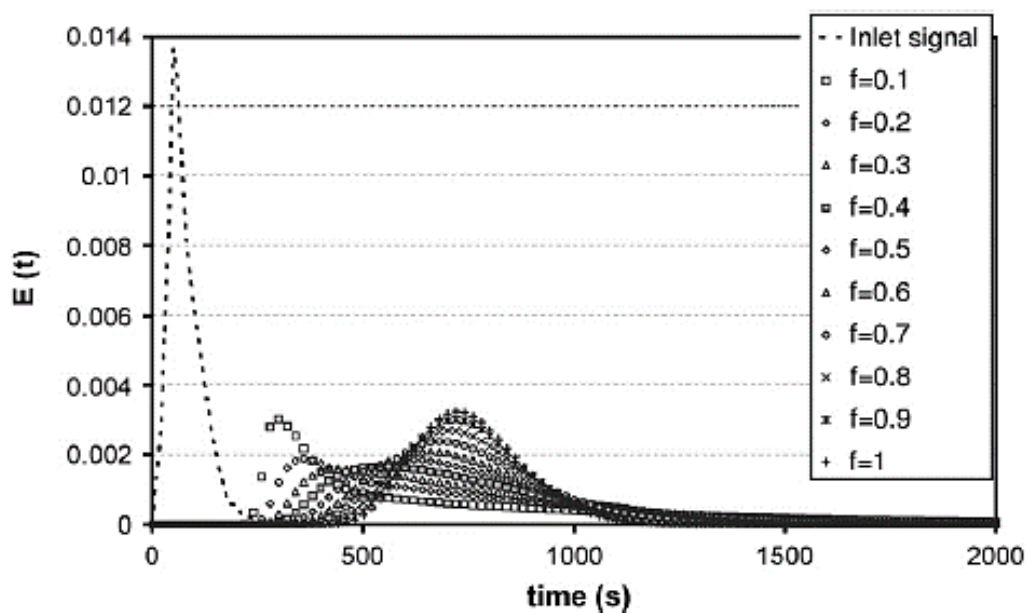
Figure 2.6: Effect of Wetting Efficiency on the Exit Age Distribution

2.2.3 Application of RTD theory to the estimation of wetting efficiency

The tracer technique is the most popular for the determination of wetting efficiency as the actual bed is under operating conditions. It consists in producing a step impulse of a tracer and analysing the time

distribution of concentration at the outlet. From RTD variance, particle effective diffusivities for the reactor operating with a full liquid phase flow in the absence of the gas and in the partial wetting regime can be calculated (Julcour-Lebigue, 2007). Wetting efficiency is found to play a similar role as external mass transfer or diffusion: the lower it is, the wider the response curve is. According to Julcour-Lebigue (2007) it can be said that tracer method may be performed to derive wetting efficiency in usual low axial dispersion conditions.

2.3 Modification of Surface Characteristics of Polymeric Materials

With respect to material chemistry it is commonly known that hydrophilic surfaces are more beneficial to liquid phase systems than hydrophobic surfaces. Therefore, in this case an improvement of the wetting and efficiency of the column can be brought about by using packing material that is hydrophilic in nature. Keeping this in mind, it is known that most polymeric materials such as polyethylene (PE), polyvinylidenefluoride (PVDF) and polypropylene (PP) are less favourable than glass and metal packing because they are weakly hydrophilic. However, of these polymers, polypropylene is superior regarding mechanical strength, chemical stability, thermal and chemical resistance and low cost (Ahsani et al, 2015). Despite the above beneficial properties, polypropylene lacks polar functional groups making it very hydrophobic. Modification of the polypropylene surface can thus be performed to enhance its hydrophilicity and make it a well-suited material for packing boasting better chemical resistance, good separation performance and better adaptability to chemical systems.

Membrane modification can be carried out in a variety of ways. This investigation incorporates an inorganic silica nanoparticle phase onto the surface of the polypropylene. Before the formation and coating of silica nanoparticles can be done, the polypropylene needs to be pre-treated by oxidation to create hydroxyl functional groups (-OH) on the polymer surface. This is done using a volume ratio of 3:1 sulfuric acid (H_2SO_4) and hydrogen peroxide (H_2O_2) solution called the Piranha solution. The presence of the -OH groups allows for the chemical bonding of silane agents to the polymer surface as stated by Ahsani et al (2015).
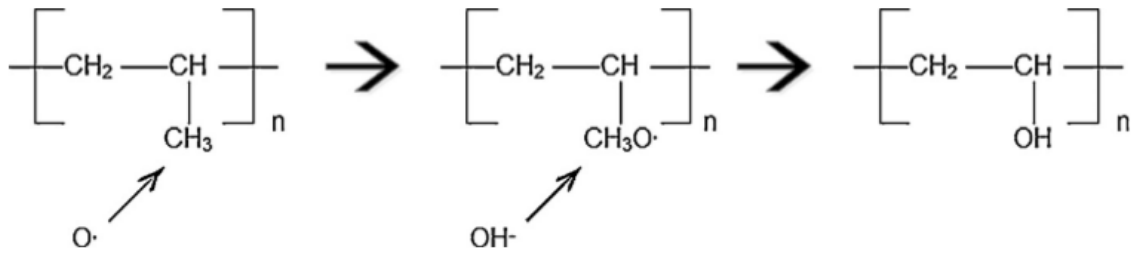
Figure 2.7: Oxidation of Polypropylene with the Piranha Solution (Ahsani et al, 2015).

Figure 2.7 above, shows the oxidation process in which hydronium ions, bisulphate ions and reactive oxygen was produced. The reactive oxygen further reacts with water molecules to form a hydroxyl ion.

The Stober process is employed for the formation of monodispersed silica nanoparticles via hydrolysis of alkyl silicates and polycondensation of silicic acid in an alcohol solution where ammonia is used as a catalyst as stated by Ibrahim et al (2010). An ex situ approach is used. During the hydrolysis reaction, a tetraethylorthosilicate (TEOS) pre-cursor is dissolved in a methanol solution and contacted with the ammonia catalyst. This completes the synthesis of silica nanoparticles. The pre-treated polypropylene packing with hydroxyl groups reacts well with the prepared silica nanoparticles through polycondensation at a fixed temperature of 40 °C to complete the modification. Figure 2.8 shows the hydrolysis and polycondensation reaction mechanisms of TEOS.
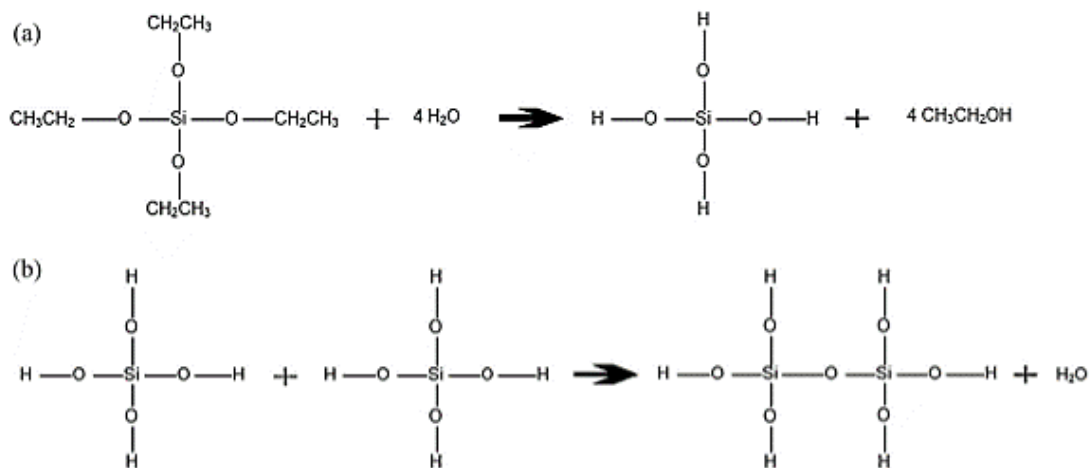
Figure 2.8: (a) The Hydrolysis Mechanism. (b) Polycondenstion to Coat the Polypropylene Packing (Ahsani et al, 2015).

Figure 2.9 below, shows a schematic representation of the formation of silica nanoparticles on the polypropylene surface after treatment with the Piranha solution. The figure shows the silica oligomer formation followed by the chemical bonding of the formed silica nanoparticles to the treated surface consisting of hydroxyl functional groups ready for attachment. The solid bar in the figure represents the polypropylene surface. The last step indicates the final coated polypropylene surface.
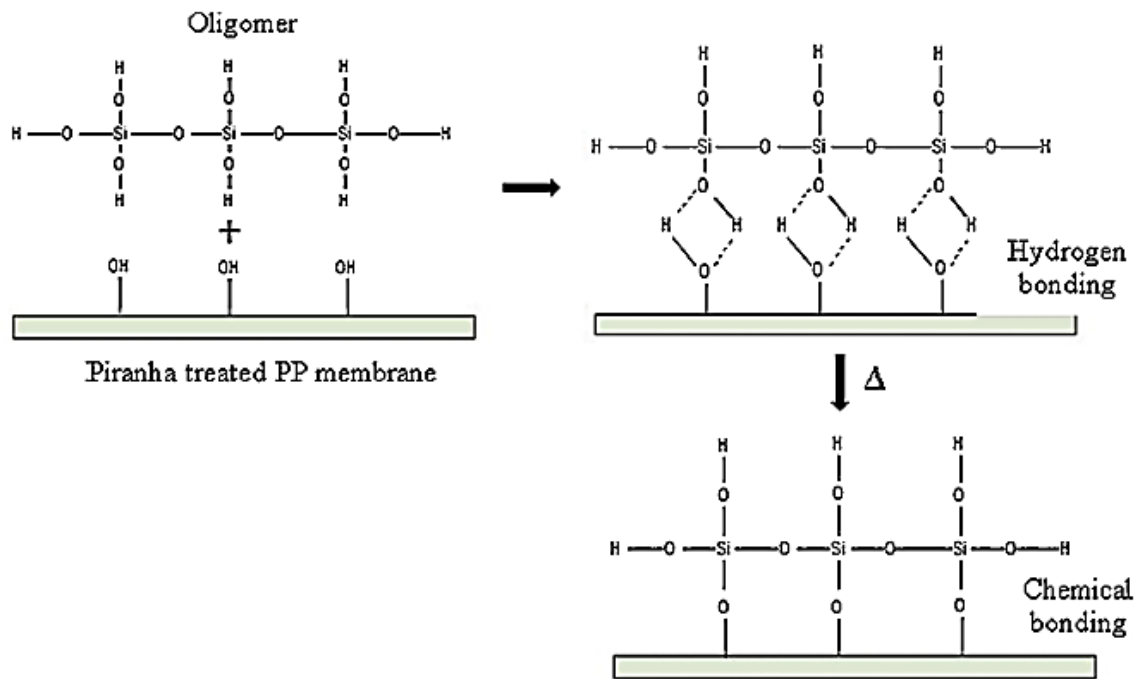
Figure 2.9: Schematic Representation of Silica Nanoparticle Formation on the Treated Polypropylene Surface (Ahsani et al, 2015).

2.4 Analytical Techniques

2.4.1 Contact Angle Measurements

The contact angle is defined as the angle formed by the intersection of the liquid-solid interface and the liquid-vapour interface attained geometrically when a tangent is applied from the contact point along the liquid-vapour interface. Contact angle measurements usually form the primary data used when determining the wettability of materials as they indicate the degree of wetting when a solid and liquid interact (Yuan et al, 2013). Contact angle measurements can be performed by observation of the angle formed by a sessile liquid droplet, usually water, and a solid surface using a high-powered microscope or a telescope goniometer.

Resulting small contact angles, less than 90 °, are an indication of high wettability as the liquid spreads over a large area of the surface of the solid. Large contact angles, greater than 90°, indicate a low wettability when the liquid beads on the surface minimizing the area of contact. This can be seen in Figure 2.10.
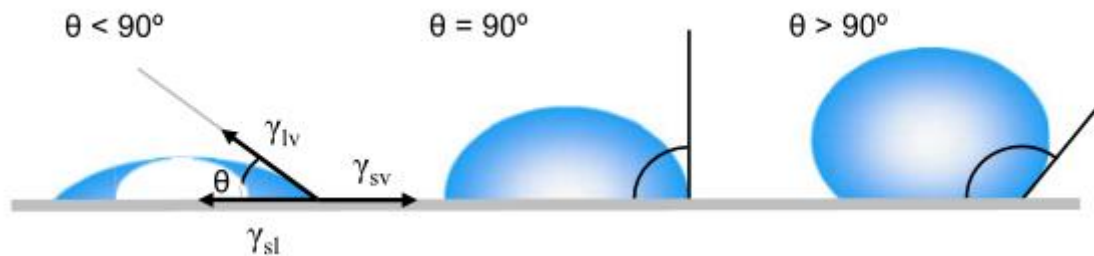
Figure 2.10: Contact Angles Formed by a Sessile Liquid Droplet on a Smooth Solid Surface

However, if a telescope goniometer is not available a high-power microscope such as the Nikon AZ100 High Power microscope and appropriate software such as Nikon Imaging Software (NIS) Elements can be used. The microscope and software is able to handle multi-dimensional imaging with supporting functions to capture and display images to be analysed.

2.4.2 Scanning Electron Microscope (SEM) Imaging

A scanning electron microscope is used to characterize microscopic morphology or topography of a surface in a high resolution, three-dimensional format. The microscope uses focused beams of electrons to scan samples and provide information on their structure. In this investigation, SEM images will provide insight on the physical deposition of silica nanoparticles on the surface of the polypropylene packing material. The images will also validate the change in contact angle between the unmodified and modified polypropylene. Large deposition of nanoparticles indicates a well-coated surface corresponding to a small contact angle and improved wetting efficiency.

2.4.3 Titration Method

During an acid-base titration, the pH changes in a characteristic way. A pH curve is found if the pH of the solution being titrated is plotted against the volume of solution added. Some typical pH curves in which 0.1M solutions of various acids and bases are titrated together are shown in figures 2.11 and 2.12 (below). The Ka for the weak acid is 4.75 (like ethanoic acid), and the Ka for the conjugate acid of the weak base is 9.25 (like NH_4^+, the conjugate acid of ammonia).
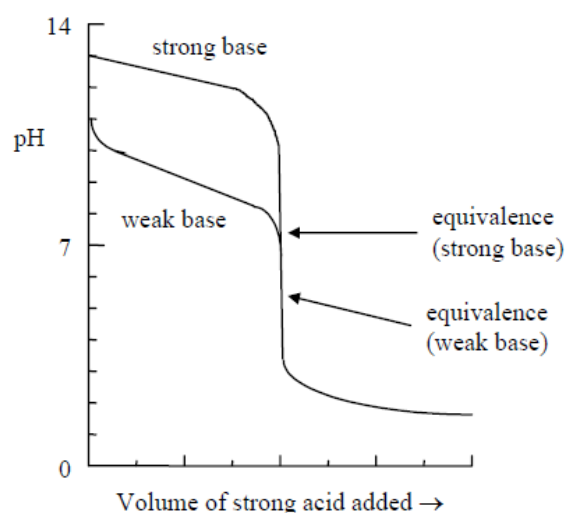
Figure 2.11: The titration curves of a strong acid (e.g. HCl) added either to a strong base (e.g. NaOH) or to a weak base (e.g. NH3).
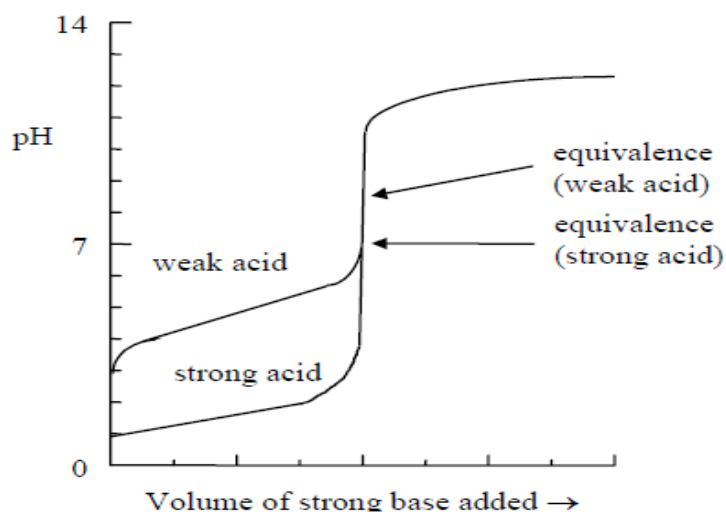
Figure 2.12: The titration curves of a strong base (e.g. NaOH) added either to a strong acid (e.g. HCl) or to a weak acid (e.g. CH3COOH).

20

2.4.4 Gas Analysers

Gas analysers are one of the safety instruments used in many industries and pharmaceutical companies to maintain adequate safety in the work place, they are used to find out the gases in the atmosphere and the signals are displayed on the monitor, analysers or detectors gives complete information on different gases including sulphur dioxide, oxygen, carbon dioxide, nitrogen dioxide, and methane, as well as their physical factors such as flow rate and pressure and temperature.

Electrochemical gas analysers measure the concentration of a target gas by oxidizing or reducing the target gas at an electrode and measuring the resulting current. The sensors contain two or three electrodes, occasionally four, in contact with an electrolyte. The electrodes are typically fabricated by fixing a high surface area precious metal on to the porous hydrophobic membrane. The working electrode contacts both the electrolyte and the ambient air to be monitored usually via a porous membrane. The gas diffuses into the sensor, through the back of the porous membrane to the working electrode where it is oxidized or reduced. This electrochemical reaction results in an electric current that passes through the external circuit.

CHAPTER 3: EXPERIMENTAL METHODS

3.1 Part A – Determination of wetting efficiency of polymeric packing

3.1.1 Experimental Setup

To carry out this investigation on the wetting efficiency of polypropylene packing modified by silica nanoparticles using a simultaneous tracer technique, the appropriate equipment had to be designed, sourced and assembled to form a functioning packed column with a liquid inlet of deionised water over a packed bed of glass or polypropylene Raschig rings. Raschig rings were selected due to it being simple, cost effective and having a wealth of literature available. An injection point / septum was positioned on the liquid line as the tracer injection point. A conductivity meter was used to measure the change in conductivity once the salt tracer solution was injected. Concentration was inferred from conductivity and used to determine the residence time distribution and exit age distribution. The setup can be found in the Chemical Engineering Laboratory at the University of KwaZulu-Natal. Figure 3.1 shows the types of packing used and Figure 3.2 shows the equipment setup in this investigation.

A 50 mm inner diameter glass column was packed to a height if 370 mm with glass, unmodified or modified polypropylene Raschig rings for each trial. The inner diameter of the Raschig rings were 5 mm and 7 mm for glass and polypropylene, respectively, with a length of 8 mm. These dimensions were chosen due to the ratio of the diameter of the column to the diameter of the packing. A ratio much smaller than 10 may create a strong wall effect (Rase 1977) which will disrupt liquid and gas flows. A liquid inlet line was positioned above a liquid distributor, inserted 70 mm above the packing to insure uniform distribution of fluid. Silicon tubing was used to carry deionized water from a 25 L water tank. A Heidolph peristaltic pump was used to pump water at 830 ml/min from the tank to the column. A Crison conductivity meter recorded changes in conductivity of the fluid flowing over a glass probe placed in a Perspex holder at the column outlet. Conductivity as a function of time was logged onto a laptop using a software called HyperTerminal

Figure 3.1: Glass, Unmodified and Modified Polypropylene Raschig Rings.
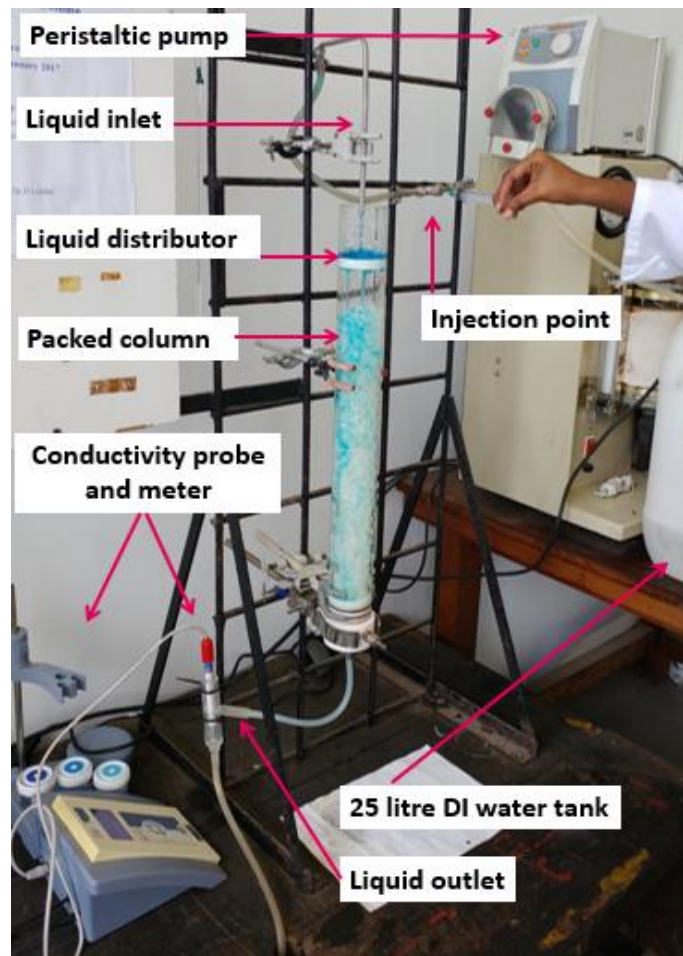
Figure 3.2: Experimental Setup in Laboratory

3.1.2 Materials and Methods

The materials used for Part A of the experiment were 10 g fine table salt, deionized water and blue inkpad dye.

<u>Preparation of Standard Solution</u>

To begin 10 g fine white table salt was weighed out in a clean beaker and 50 ml deionised water was added. The solution was swirled to dissolve the salt, decanted into a volumetric flask and topped to the 100 ml graduation with deionised water. The flask was then inverted several times to properly mix the solution. A portion of the solution (approximately 40 ml) was poured into a smaller beaker and 4 drops of blue dye was added to improve the visibility. The dyed solution was used as the tracer injection in each run.

Conductivity Meter Calibration

For the experimental work to be performed, the Crison conductivity meter needed to be calibrated. Firstly the conductivity of three standard solutions of known conductivity, available with the Crison conductivity meter, were measured. The value displayed on the conductivity meter was then plotted against the actual conductivity of the standard solution as can be seen in Figure C-1 in Appendix C. A line of best fit was used to determine the relationship between the actual and displayed conductivity. The second part of this calibration required 0; 2.5; 5 and 7.5 ml aliquots of a 1.71 M NaCl solution to be added to 100 ml deionised water to prepare solutions of varying salt concentration. The conductivity of these solutions with known concentrations was then measured. The displayed conductivity was then used together with the calibration relationship in Figure C-1 to determine the actual conductivity. The actual conductivity obtained was plotted against concentration as seen in Figure C-2. A line of best fit was used to determine the relationship between conductivity and concentration. A residual Plot, found in Figure C-3 shows the dispersion of the calibration results about the x-axis.

Experimental Procedure

Wetting efficiency is strongly affected by hydrodynamic properties, therefore, after varying the flowrate, the operating flowrate was selected to be 555 ml/min. The salt solution was prepared as a 1.71 M NaCl (table salt) solution with an addition of blue dye to improve visibility as the solution flowed through the column. This choice was made due to the cost effectiveness, non-reactive behaviour, availability and safety of the components. Three runs were performed for each type of packing.

A 25 L water tank was used to collect deionised water from the deionised water reservoir in the Analytical Laboratory. The conductivity meter, peristaltic pump and laptop were appropriately positioned and plugged on. Bearing in mind to keep all cables tidily away from sources of liquid and pathways to prevent accidents. The glass conductivity probe was placed into its Perspex holder, HyperTerminal was started on the laptop and the conductivity meter was switched on to begin conductivity measurements. The silicon tubing was fully submerged in the deionised water tank and the peristaltic pump was set to 100 rpm to maintain a flowrate of 555 ml/min. The system was flushed with a small amount of deionised water and time was allowed for the conductivity readings to stabilise around $0.3\ \mu S - 0.34\ \mu S$. The start time and stable value for each run were recorded. 10 ml of the dyed standard solution was syringed and injected through the septum into the liquid line. The data logger on the laptop was monitored. When the conductivity readings reached approximately

$0.3\mu S - 0.34\,\mu S$ again, the program and peristaltic pump were stopped. This usually occurred approximately 3 minutes after the time of injection. Once all data has been recorded the column was drained to remove any remaining liquid. The data obtained was transferred to Microsoft Excel where it was used to determine the residence time and exit age distribution allowing for the estimation of wetting efficiency for each type of packing. Valuable equipment such as the conductivity meter, glass probe and laptop were packed away. The remaining water in the tube was dispensed back into the tank and the pump was unplugged.

3.1.3 Supporting Experimental Procedures

Modification of Polypropylene by Coating with Silica Nanoparticles

Treatment with the Piranha solution:

The Piranha solution was prepared by adding 200 ml H_2O_2, dropwise from a burette, to beaker containing 600 ml H_2SO_4 and was performed in a fume hood. The polypropylene packing was immersed in the solution for 3 hours. The packing was then immersed in de-ionized water for 10 minutes and left to dry on a sheet of paper towel for 2 hours at room temperature.

Figure 3.3: Polypropylene Packing Immersed in the Piranha Solution

Preparation of silica nanoparticles:

A solution consisting of 10.8 ml H_2O, 12 ml NH_3 solution and 600 ml CH_3OH was prepared in a round bottom flask positioned on a heating mantle. A hole was drilled into a rubber stop and a thermometer

was inserted to monitor the temperature and maintain it at 40 °C when used to seal the flask. 66 ml of tetraethylorthosilicate (TEOS) was added dropwise to the solution and stirred vigorously using a magnetic stirrer. The flask was then sealed and the solution was left to stir intensively on the heating mantle at 40 °C for 5 hours under reflux.

Coating of polypropylene packing with silica nanoparticles:

The flask containing the silica solution was removed from the heating mantle. Polypropylene packing was poured into the flask and the rubber stop was replaced. The flask was then placed in a water bath at 40 °C for 15 hours under reflux as can be seen in Figure 3.4. After 15 hours, the packing was removed from the solution and placed on trays and left to dry in an oven at 100 °C for 6 hours. The packing was then placed in an ultrasound bath for 15 min and then returned to the oven at 100 °C for 1 hour. This resulted in polypropylene packing modified by coating with silica nanoparticles. The modified packing was then inserted into the glass column and the experimental procedure was followed to continue the investigation.

Figure 3.4: Preparation and Coating with Silica Nanoparticles under Reflux.

Contact Angle Measurement

Contact angle measurements were done on unmodified and modified polypropylene Raschig rings. A Nikon AZ100 High Power Microscope and NIS Elements software, at the University of KwaZulu-Natal Mechanical Engineering Metallurgy Department, was used. Four measurements were done for both types of polypropylene packing and the average angle was reported.

The measurement procedure began with the Nikon AZ100 High Power Microscope, aiding Nikon light and computer being switched on. One polypropylene (unmodified or modified) Raschig ring was placed on a flat raised surface under the lens. The lens of the microscope was adjusted to focus and meet a clear visual preference. A small drop of water was carefully placed on the wall of the Raschig ring using a thin glass rod. It is important to note that the drop must remain in position and not fall off the packing. Once the drop was in position a photo was taken by the microscope and transferred to the computer. Using the NIS Elements software, tangents were drawn to the solid surface and to the outer dome of the water droplet. The angle was then measured electronically and manually recorded. This was repeated 4 times for each type of packing. On completion, the microscope, aiding light and computer were switched off.
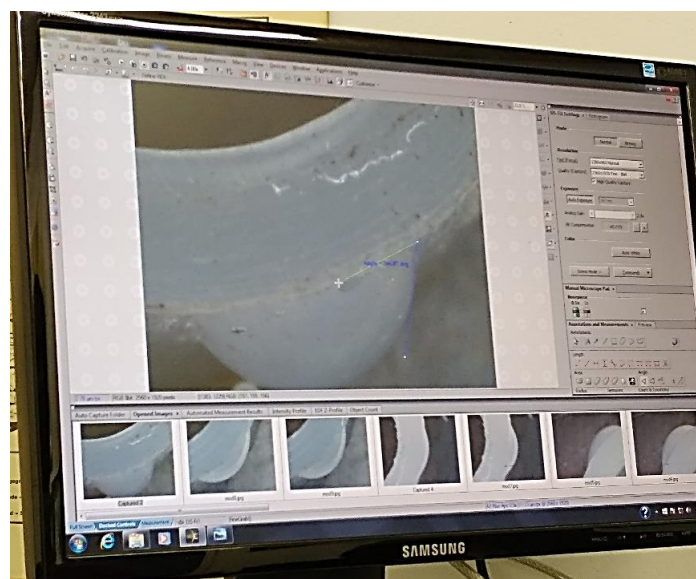
Figure 3.5: NIS Elements Software used to measure the contact angle.
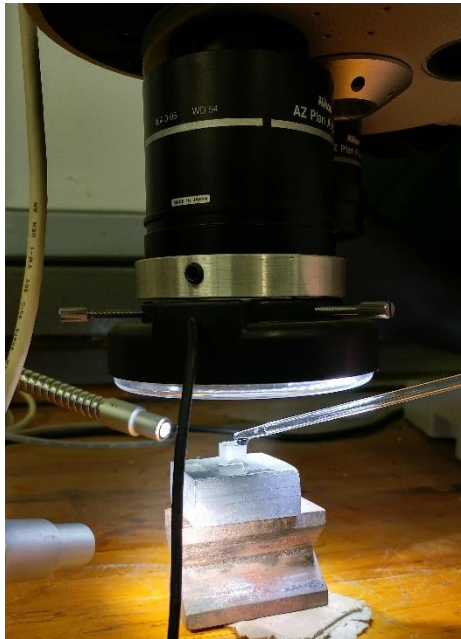
Figure 3.6: Sample under the Microscope.

Scanning Electron Microscope Imaging

The following process was carried out to obtain the SEM images for each sample of unmodified and unmodified polypropylene Raschig rings.

Gold plating of samples to further improve conductivity for the electron beams to improve image quality was done in a machine called a "gold squatter" machine, shown below in Figure 3.7. This took approximately 10 minutes. Aluminium stubs were used to hold the samples while carbon based two-way tape was used and placed on top of the aluminium stubs. The samples were placed on the tape in the direction of which it is to be analysed. For example, the plastic samples were analysed on the inner cylinder so it was placed facing upwards between the aluminium stubs. Graphite in xylene solution was used to fill gaps and improve the conductivity. Time was allowed for the sample to dry and were then analysed with the images being captured.

For conventional imaging in the SEM, specimens must be electrically conductive, at least at the surface, and electrically grounded to prevent the accumulation of electrostatic charge (Vishal Bharuth).

Figure 3.7: "Gold-Squatter" used to plate samples to improve conductivity.

3.2 Part B - Absorption Performance

3.2.1 Experimental Setup

To carry out this investigation on the absorption efficiency of different packing materials the appropriate equipment had to be designed, sourced and assembled to form a functioning packed column. The experimental setup from Part A was used with some modifications. The injection point was removed to ensure that there were no leaks in the system. An inlet gas stream was added to the bottom of the column coming from a gas cylinder which was controlled by passing through a rotameter. The column and Raschig rings dimensions were unchanged while the packed height was changed to 90 and 280 mm for different runs. The liquid and gas flows were also varied to investigate their effects on the absorption performance. Silicon tubing was used to carry deionized water from a 25 L water tank. A Heidolph peristaltic pump was used to pump the water at 122, 390 or 555 ml/min from the tank to the column. This fluid then passes over the various types of packing at various flowrates of gas.

Two analytical methods were used to analyse the carbon dioxide being absorbed. The first being the titration method which required the outlet liquid stream to being collected. Therefore, the outlet liquid stream leaves the glass column through a silicone outlet pipe located at the bottom of the column and passes into a solution of sodium hydroxide. This solution then reacts with the carbon dioxide and water to form a mixture of sodium carbonate and excess sodium hydroxide in solution. Next the new solution was titrated with a solution of dilute hydrochloric acid, in the presence of a portable pH meter. The results were then recorded and data analysis were undertaken on these. The method was fairly accurate for higher concentrations of carbon dioxide but for low concentrations a new analytical method had to be used.

The second method required using the gas analyser which required the inlet and outlet gas stream to be measured. The main modification that had to be made was ensuring the column was a gas tight system and no gas could escape before measurements were made. The column was sealed using a Teflon cap with two holes drilled in it. The first hole was for the inlet water stream and was drilled to the exact size to prevent any leaks. The second hole was for the gas analyser to fit in. Checks were made to ensure that no leaks present. This method was easy to analyse using the principle of carbon dioxide in minus out equals amount of carbon dioxide absorbed.
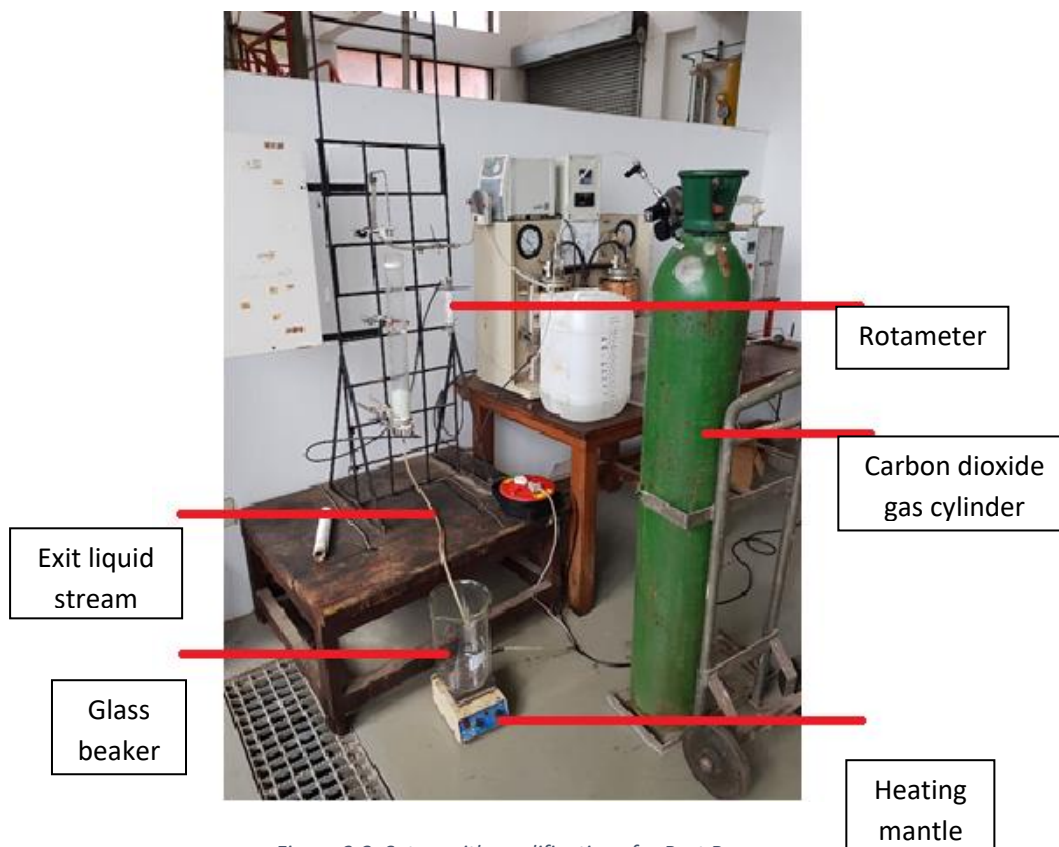
Figure 3.8: Setup with modifications for Part B

3.2.2 Materials and Methods

The materials used in Part B of the experiment include deionised water concentrated hydrochloric acid, sodium hydroxide pellets, nitrogen gas and carbon dioxide gas.

Preparation of Sodium Hydroxide Solution

Different molar concentrations of sodium hydroxide were used in different in experiments. For the 0.1 M concentration solution, 2 litres of deionised was measured out and put into a beaker. The sodium hydroxide pellets available were 40g per a 1 M solution therefore 8g were used to make 2 litres of 0.1 M concentration. The beaker of water was placed on a heating mantle with the heat off and stirrer turned on to a medium speed. A magnetic stirrer was placed in the beaker and the sodium hydroxide pellets were added. Once the pellets were dissolved the solution was left to cooled. A pH meter was then used to check if the concentration was accurate and then stored in a volumetric flask

until used in the experiments. To make the 0.02 M concentration solution, the same procedure was followed with the only change being that 0.4g of sodium hydroxide pellets were used.

Preparation of Hydrochloric Acid Solution

Different molar concentrations of hydrochloric acid were used in different in experiments. A 12 M concentration of hydrochloric acid was available in the laboratory. Initial a 1 M solution was made and was then diluted down to the 0.1 M and 0.01 M solutions needed in the experiments. The 12 M hydrochloric acid forms acidic mist when opened therefore this was performed under a fume hood with gloves. To begin it was calculated that 8.33 mL of concentrated hydrochloric was needed to make a 1 litre solutions. 991.67 mL of deionised was measured out and added to a volumetric flask. The 8.33 mL of the 12 M hydrochloric acid was measured and added to the hydrochloric acid. The volumetric flask was then shaken for a minute to allow the solution to be mixed. A pH meter was then used to check if the concentration was accurate and the 1 M solution was then stored. For the 0.1 M solution, 10 mL of 1 M hydrochloric acid was added to 90 mL of deionised water while for the 0.01 M solution, 1 mL of 1 M hydrochloric acid was added to 99 mL of deionised water to make 100 mL solutions for each run it was used for. Before use a pH meter was then used to check if the concentrations were accurate.

Rotameter Calibration

A bubble flow column was obtained and cleaned. A liquid soap solution was made using regular dish washing soap and water. The gas inlet to the absorber was removed and connected to the bubble flow column and the connection was secured with insulation tape to avoid leakage. The bulb at the bottom of the bubble flow column was filled with the liquid soap solution. The gas was turned on and the bulb was squeezed to allow for bubbles to form. The inlet gas flowrate was held constant and the bubbles tracked up the column for a certain distance and the time taken was recorded. The inlet gas flowrate was then changed and the procedure of tracking a bubble for a particular distance and recording the time repeated. This was done for several different gas flowrates. A calibration curve was plotted and the respective gas flowrates were determined as can be seen in Appendix C.

Experimental Procedure for pH method

During the initial phase of the experiment, the results obtained were inconsistent with the expectations from theory. These discrepancies were attributed to the flowrate of carbon dioxide and

the initial concentrations of the sodium hydroxide and hydrochloric acid solutions. It was then decided that lower concentrations of both solutions should be used for greater accuracy and to enable easier location of the endpoints of the titration. Once a workable procedure and concentration of solutions were obtained, runs were carried out in which the flowrates of the carbon dioxide were varied for each packing type.

A 25 L water tank was used to collect deionised water from the deionised water reservoir in the Analytical Laboratory. The pH meter, peristaltic pump, magnetic stirrer and laptop were appropriately positioned and plugged on. Bearing in mind to keep all cables tidily away from sources of liquid and pathways to prevent accidents. The silicon tubing was fully submerged in the deionized water tank and the peristaltic pump was set to the required speed for each run. Thereafter, the carbon dioxide was let into the column at a pressure of 1 atm, and the flowrate that was required for the run. The flows of gas and deionized water were allowed to run for 5 minutes to allow for a steady state and complete saturation of carbon dioxide and wetness of the packing to be achieved. Thereafter, the run was started and the flows were left at their set values for the time required for the run, the solution exiting the column was collected in the 5000 mL beaker, while simultaneously being mixed with the sodium hydroxide solution by the action of the magnetic stirrer. Once the run was completed, the flows of liquid and gas were shut, and 100 mL of the sodium carbonate and sodium hydroxide mixture were removed from the large 5000 ml beaker and placed into a smaller beaker. The pH meter was then inserted into this beaker and an initial reading of the value of the pH was taken. Thereafter, 100 mL of the required hydrochloric acid solution was decanted into a separate beaker. This was then pipetted into the beaker containing the sample from the column. As this occurred, measurements of the pH were recorded onto an excel spreadsheets at varying intervals of volume added. The reason for the variation in the volumes of hydrochloric acid added between measurements was to allow for 'magnification' of the results, allowing the end points to be obtained more easily. Valuable equipment such as the pH meter, magnetic stirrer and laptop were packed away. The remaining water in the tube was dispensed back into the tank and the pump was unplugged. After the runs for each packing were completed, the gas was switched off and the top of the column opened and the old packing replaced with a new type.

Experimental Procedure for Gas Analyser method

Deionized water was collected and stored in a 25 L water tank. The gas analyser was connected and switched on to allow for it to calibrate, taking approximately 40 minutes. The outlet gas line was connected to the analyser and insulation tape used to ensure there were no leaks. Thereafter the gas

was fed into the column at flowrate needed for the run. The gas would flow until the CO_2 value in the column increased and then stabilized, this value was then recorded (approximately 5 minutes). Thereafter, the run was started and the water allowed to flow at the required speed. The stable CO_2 value after a period was recorded and the water switched off. Three runs were performed for each packing at the required flowrate and the inlet and outlet CO_2 values recorded. After the runs for each packing were completed, the gas was switched off and the top of the column opened and the old packing replaced with a new type. At the end of each day the gas analyser was switched off and allowed to save the data following which it was dissembled and stored away. The gas tanks were closed and checked for any possible leaks.

3.2.3 Supporting Experimental Procedures

Selection of Absorption System

For the absorption experiments in this study, a system of water and carbon dioxide was selected to be used as it is a very simple and non-toxic system. Water is also a very common absorbent used in absorption systems. The main reason this system was selected is that it can be analysed using the titration method. The amount of carbon dioxide being absorbed into the water could be quantified as it reacts with sodium hydroxide, a strong base. This new solution could be titrated against a strong acid, hydrochloric acid to determine the amount of carbon dioxide being absorbed.

Titration Method

During an acid-base titration, the pH changes in a characteristic way. A pH curve is found if the pH of the solution being titrated is plotted against the volume of solution added. A typical pH curves in which 0.1M solutions of various acids and bases are titrated together is shown in figure 3.9.
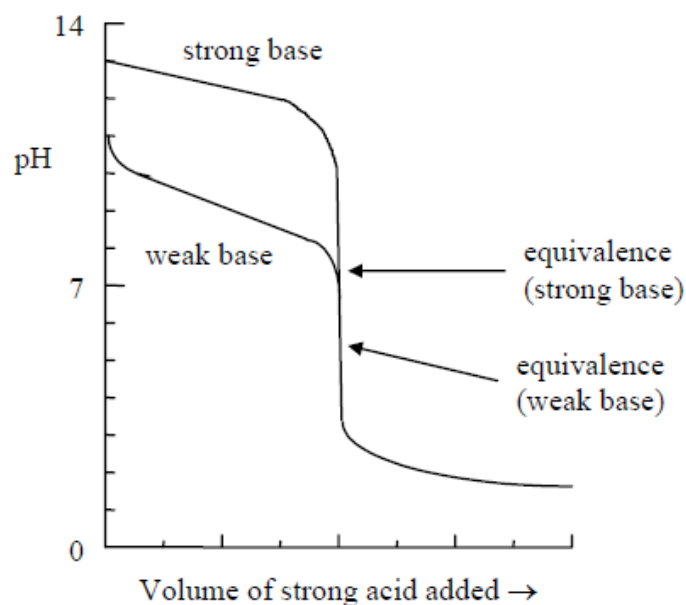
Figure 3.9: The titration curves of a strong acid (e.g. HCl) added either to a strong base (e.g. NaOH) or to a weak base (e.g. NH3).

For this investigation sodium hydroxide was selected as the base as it reacts with the carbon dioxide which is the gas being absorbed. To determine the amount of carbon dioxide being absorbed, excess sodium hydroxide was used to ensure all the carbon dioxide was reacted. Hydrochloric was selected to be used as the base for this investigation as it is a strong acid which would work well with sodium hydroxide as it is a strong base. The pH readings from the titration was plotted against the volume of hydrochloric acid used to form the titration curve. The results were sent through a Matlab code to determine the inflection or turning points. As can be seen in figure 3.9, there will be two points. The difference between the x-axis values of these points is the volume (V) of hydrochloric acid used to neutralise the remaining sodium hydroxide in the solution. The concentration (C) of hydrochloric acid used in the run was known and equation 3.1 was used to determine the number of moles (n) of hydrochloric acid used.

$$V_{HCl} \times C_{HCl} = n_{HCl} \tag{3.1}$$

The number of moles of hydrochloric acid used to neutralise the sodium hydroxide is equal to the number of moles of sodium hydroxide remaining as can be seen in equation 3.2.

$$n_{HCl} = n_{NaOH} \tag{3.2}$$

Since only a 100 mL sample of the sodium hydroxide and sodium carbonate solution was used, the number of moles of sodium hydroxide had to be scaled up to determine the total amount of unreacted sodium hydroxide for the run as can be seen in equation 3.3.

$$\textit{Moles of NaOH remaining} = n_{NaOH} \times \frac{\textit{Total volume of solution}}{100} \qquad (3.3)$$

Next the initial amount of sodium hydroxide for the run was calculated using equation 3.4.

$$\textit{Initial moles of NaOH} = C_{NaOH} \times V_{NaOH} \qquad (3.4)$$

To get the number of moles of sodium hydroxide reacted for the run, we used equation 3.5.

$$\textit{Moles of NaOH reacted} = \textit{Initial moles of NaOH} - \textit{Moles of NaOH remaining} \qquad (3.5)$$

Now that the number of moles of sodium hydroxide reacted for the run has been calculated, the amount of carbon dioxide being absorbed in the absorption column can be determined. Using the following chemical reaction shown in equation 3.6, the stoichiometric relationship between carbon dioxide and sodium hydroxide is 1:2. This means the number of moles of carbon dioxide absorbed is half the number of moles of sodium hydroxide being reacted as can be seen in equation 3.7.

$$2NaOH + CO_2 \rightarrow Na_2CO_3 + H_2O \qquad (3.6)$$
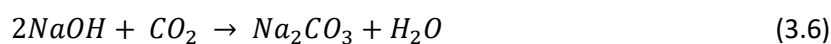
$$\textit{Moles of } CO_2 \textit{ absorbed} = \frac{\textit{Moles of NaOH reacted}}{2} \qquad (3.7)$$

3.3 Experimental Design

Table 3.1: Details of the experiments conducted for parts A and B.

Runs Performed	Packing Height (mm)	Liquid Flowrates (mL/min)	Vapour Flowrates (cm^3/min)	Carbon Dioxide Concentration (%)	Sodium Hydroxide Concentration	Hydrochloric Acid Concentration
Part A						
RTD	380	555	-	-	-	-
Part B						
Set 1	280	122	25.38; 52.52; 74.07; 90.98	100	0.1	0.1
Set 2	90	122	118.26; 122.92; 119.40	12.7; 16; 23.8	0.1	0.1
Set 3	280	122; 390; 555	122.92	16	0.02	0.01
Set 4	90	122; 390; 555	122.92	16	0.02	0.01
Set 5	90	122; 390; 555	109.35	0.683	-	-
Set 6	90	122; 390; 555	105.56	2.167	-	-

CHAPTER 4: RESULTS AND DISCUSSION

4.1 Part A - Determination of wetting efficiency of polymeric packing

The mechanism used for the addition of silica nanoparticles onto the polypropylene Raschig rings involves the following three steps: pre-treatment of the polypropylene packing, preparation of the silica nanoparticles and coating of the polypropylene packing with silica nanoparticles. The procedure for these three steps may be found in section 3.1.3 of the report.

The accuracy of this investigation was largely dependent on the components of the experimental setup. A glass column was packed with glass, unmodified polypropylene and modified polypropylene Raschig rings for its respective runs. Silicon components and appropriate steel fittings were used to assemble this non-corrosive, aqueous system. A liquid distributor was positioned above the packing to allow for uniform distribution of liquid over the packing, dissipate fluctuations caused by pumping and to prevent channelling of the fluid. A peristaltic pump was selected to pump deionised water from a water tank at a lower level to a liquid inlet at the top of the column. This pump was selected due to its 'contamination-free' operation. The fluid being pumped is confined to the tubing so the pump does not contaminate the fluid and the fluid does not foul the pump. This is especially important to maintain the conductivity of the deionised water so that the only change in conductivity is caused by the injection of the tracer solution. Peristaltic pumps are also non-siphoning which prevents back flow of fluid and promotes accurate and steady dispensing into the column. Deionised water was chosen to flow through the column because it has no effect on the chemical nature of the system and has a relatively low conductivity of 0.055 µS. The reported value in this investigation increased to approximately 0.3 µS due to exposure to air when the water tank was in use. Preliminary trials were done to find the most suitable flowrate for this investigation. By controlling the size of the tubing and the speed of the pump head at 100 rpm, a metering flowrate of 555 mL/min could be achieved. This flowrate was selected because higher flowrates caused large liquid hold-up and plugging in the liquid distributor and lower flowrates caused a sputtering and trickling effect into the column.

A stimulus response technique was recommended to be used to by both Julcour-Lebigue et al (2007) and Azmi (2015) to experimentally determine the residence time distribution and ultimately estimate wetting efficiency. Numerous models, including the hydrodynamic rivulet model, and various correlations have been developed but none have accurately determined the wetting efficiency. A salt

solution was selected as the tracer to be injected into the system due to its inertness or non-reactivity, availability and detectability by conductivity measurement. The salt solution was also found to be non-fouling. Blue dye was added to improve the colour and visibility of the tracer as it flowed through the column. The blue dye had no significant effect on the conductivity of the system. The outlet conductivity was inferred as the outlet tracer concentration as a function of time. Thus, the pulse input method chosen by sudden injection into the liquid inlet stream created an appropriate pulse response in each case resulting in the development of the residence time distribution and subsequently the exit age distribution for each type of packing used.

Plastic packing is less favoured as a packing material due to its hydrophobic nature, however it does offer advantages in cost, chemical and thermal resistance and durability. It was proposed that modification of plastic packing may make it a favourable choice. A study on the fouling behaviour of silica nanocomposite modification of polypropylene membrane in purification of collagen protein by Ahsani et al (2015) was adapted and applied to modify polypropylene Raschig rings to investigate if modification would improve the wetting efficiency. The piranha solution, prepared via a highly exothermic reaction, was used to pre-treat the polypropylene Raschig rings. The pre-treatment allowed for the formation of necessary hydroxyl groups on the solid surface. Silica nanoparticles were synthesised via the Stober process due to the availability of chemicals and equipment, and used to coat the polypropylene under reflux. Reflux was employed to prevent any vaporization and gel formation of the alcohol based solution.

Three experimental runs were performed for each type of packing (glass, unmodified polypropylene and modified polypropylene) resulting in discrete concentration-time points based on the outlet conductivity and the calibration relationship. These points were used to construct the residence time distribution and exit age distribution curves found in Appendix A. The mean residence time was calculated for each type of packing using the equations previously presented. As can be seen in Figure 4.1 the mean residence time for glass and unmodified polypropylene was found to be the same, 12 s. This was found to be acceptable as both materials are considered to have weak hydrophilicity. The mean residence time for modified polypropylene packing was found to be 19 s. This means that fluid elements resided in the column packed with silica nanoparticle modified polypropylene for a longer period. The modification process was done to make the polypropylene packing more hydrophilic. By doing this, fluid elements were greatly attracted to the surface of the packing resulting in a longer mean residence time.

Table 4.1: Mean Residence Time for Glass, Unmodified and Modified Polypropylene Packing.

Type of Packing	Mean Residence Time (s)
Glass	12
Unmodified Polypropylene	12
Modified Polypropylene	19

The wetting efficiency in this investigation is an estimation obtained by comparison of experimental exit age distribution curves to a set of standard exit age distribution curves obtained from Julcour-Lebigue et al (2007) depicted in Figure 2.6. The average of the three exit age distribution curves for each type of packing was plotted and used in the above-mentioned comparison. The initial pulse or peak was ignored as it corresponded to the bulk fluid leaving the column after injection. Bulk fluid is when liquid enters the column, some of it forms a film over the packing whilst other liquid elements travel through the interstitial spaces. The second peak and its tail were of importance as they correspond to the film fluid that adhered to the packing and slowly exited the column. The average curves, focusing on the second peak and its tail, can be found in Figures 4.1, 4.2 and 4.3. The shape and position of these graphical elements were compared to curves corresponding to a specific function, f, representing the wetting efficiency. A wetting efficiency less than 0.3 is considered to be a low value (Julcour-Lebigue, 2007).
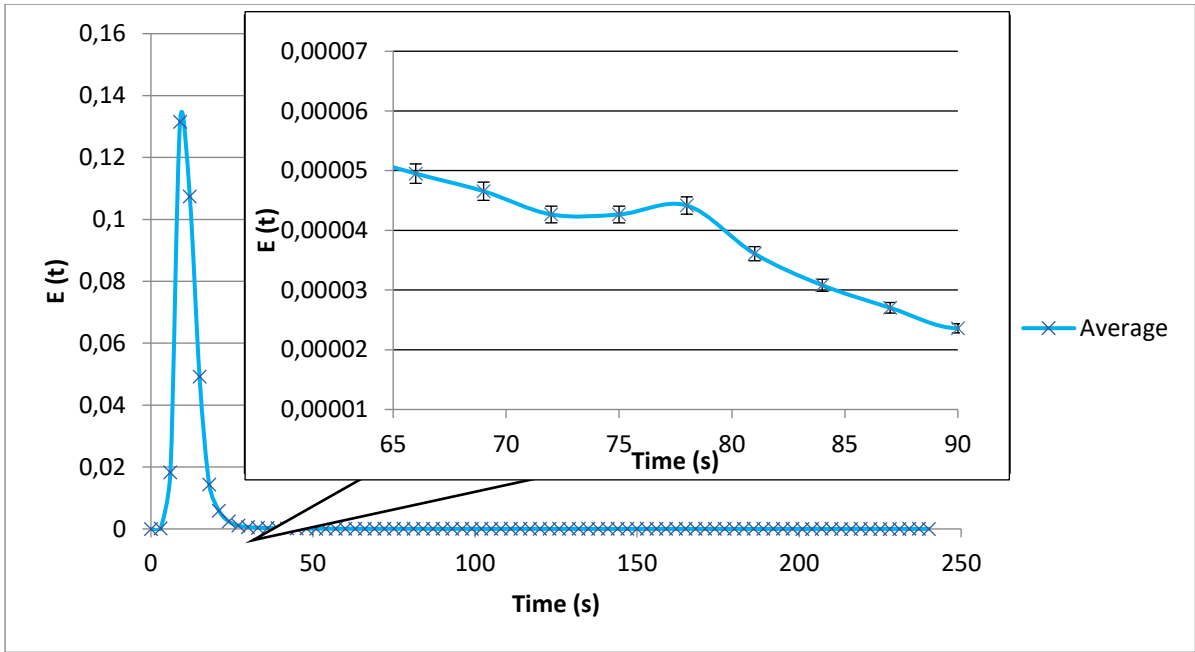
Figure 4.1: Average Exit Age Distribution Curve for Glass Raschig Rings at a packed height of 370 mm and water flowrate of 555 mL/min..
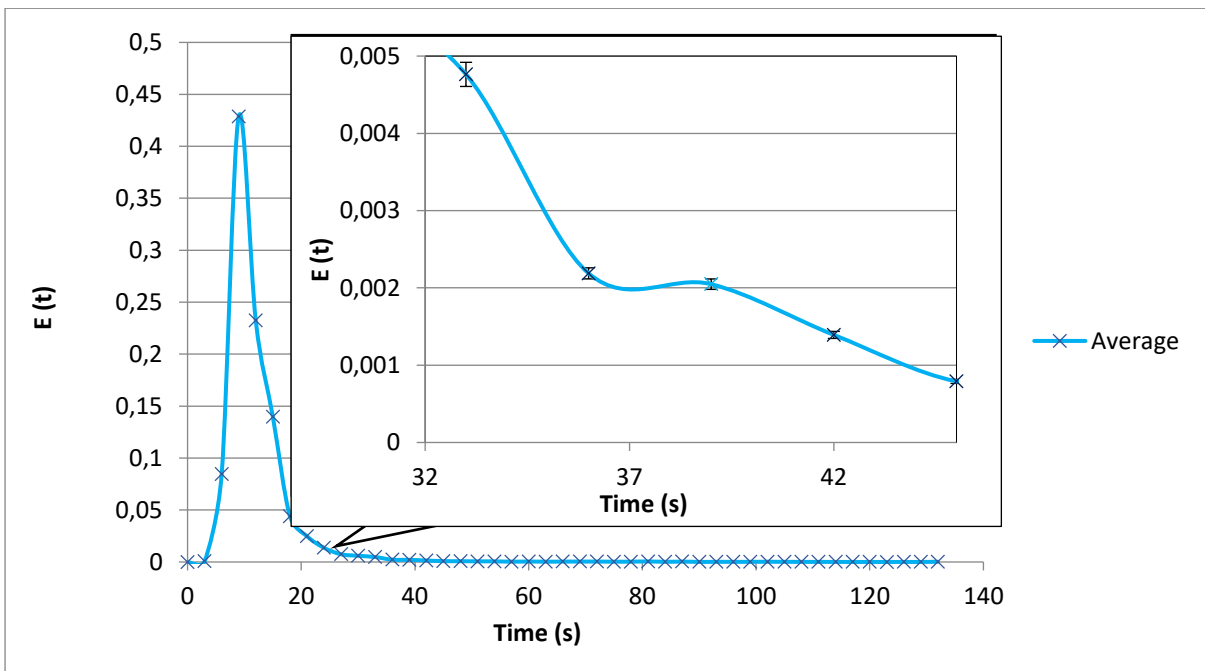
Figure 4.2: Average Exit Age Distribution Curve for Unmodified Polypropylene Raschig Rings at a packed height of 370 mm and water flowrate of 555 mL/min.
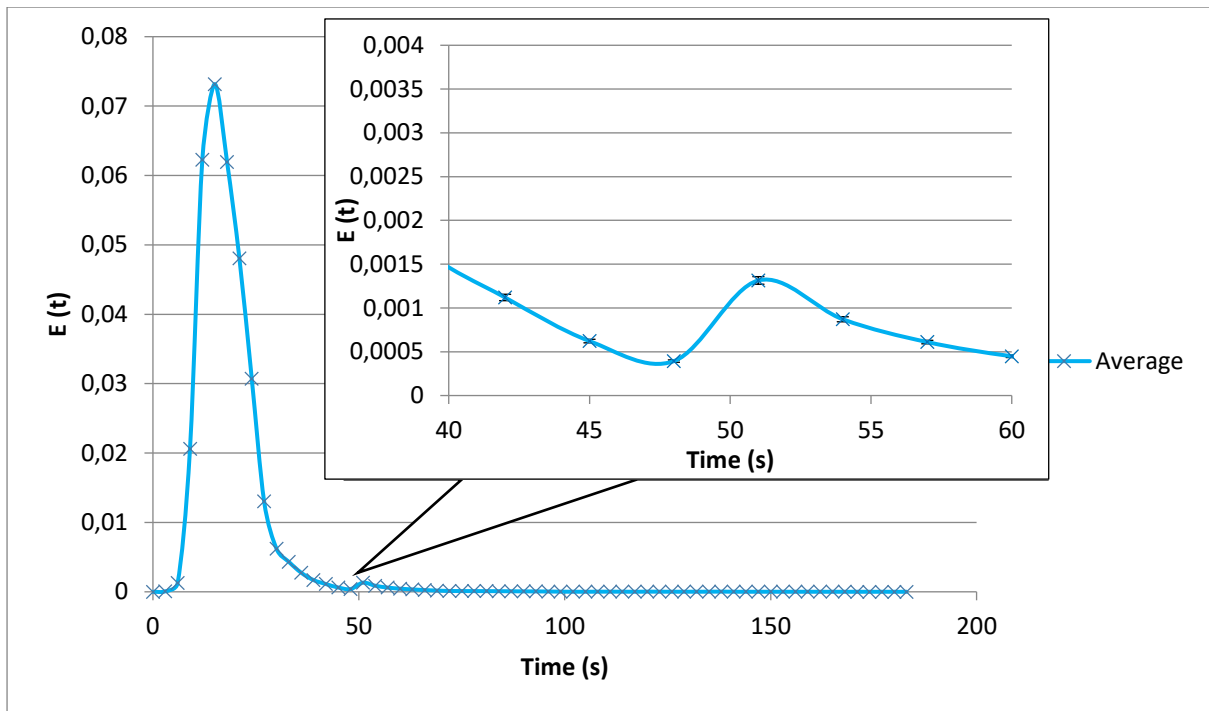
Figure 4.3: Average Exit Age Distribution Curve for Modified Polypropylene Raschig Rings at a packed height of 370 mm and water flowrate of 555 mL/min..

The wetting efficiencies of glass Raschig rings and unmodified polypropylene Raschig rings were found to be 0.3 and 0.4, respectively in table 4.2 below. Showing the unmodified polypropylene was slightly more hydrophilic than glass in this aqueous system. The wetting efficiency of modified polypropylene Raschig rings was found to be 0.8. This shows a clear improvement in wettability from unmodified to modified polypropylene. Looking at the average exit age distribution curves, it can be seen that the modified polypropylene curve widened slightly and returned to the conductivity of deionised water more gradually as compared to the slightly steeper curve obtained for unmodified polypropylene. This is because the fluid containing the salt tracer adhered to the modified surface more than to the unmodified surface and took longer to exit the column. This is an indication of the increase in hydrophilicity and improvement of wettability of polypropylene packing due to modification of its surface properties by coating with silica nanoparticles. By estimating the wetting efficiency of modified polypropylene to be higher it can be said that the modification of the polypropylene surface did prove to be advantageous.

Table 4.2: Estimated Wetting Efficiency for Glass, Unmodified and Modified Polypropylene Packing.

Type of Packing	Wetting Efficiency, f.
Glass	0.3
Unmodified Polypropylene	0.4
Modified Polypropylene	0.8

The contact angle between a sessile water droplet and the surface of the unmodified and modified polypropylene Raschig rings was measured and can be found below in table 4.3. It was advised that the glass Raschig rings were not tested as it could easily break during testing which would damage the equipment. The sessile drop technique indicates that method of placement of the drop is not dependent for the measurement, the liquid used and the surface it interacts with determines the measurements. The measurement was carried out 4 times and the average contact angle was reported in each case. The contact angle of the unmodified polypropylene Raschig ring was found to be 41.32 ° while the contact angle of modified polypropylene decreased to 37.32 °. The reason to explain the decrease in the contact angle can be due to the presence of silica nanoparticles on the surface of the modified polypropylene Raschig rings. The coating formed a layer over the surface that caused the angle at which the liquid phase meets the solid phase to decrease because of a change in the solid surface properties. It can therefore be said that modification of the polypropylene surface with silica nanoparticles has decreased the contact angle of polypropylene and improved the hydrophilicity as a lower contact angle corresponds to a higher wetting efficiency as mentioned by Yuan et al (2013).

Table 4.3: Average Contact Angle Measurements for Unmodified and Modified Polypropylene Packing.

Type of Packing	Contact Angle (°)
Unmodified Polypropylene	41.323
Modified Polypropylene	37.323

Scanning electron microscope images were taken of the unmodified and modified polypropylene surfaces. These images allow a clearer and more qualitative analysis of the extent of deposition of silica nanoparticles on the surface. Figure 4.4 shows the plain surface of the unmodified polypropylene Raschig ring. The Energy dispersive X-ray (EDX) spectroscopy results shows corresponding compositions, as can be seen in table 4.4 which validates that no silica was present on this surface. The weight sigma refers to the error in the weight percent concentration at the 1 sigma level.
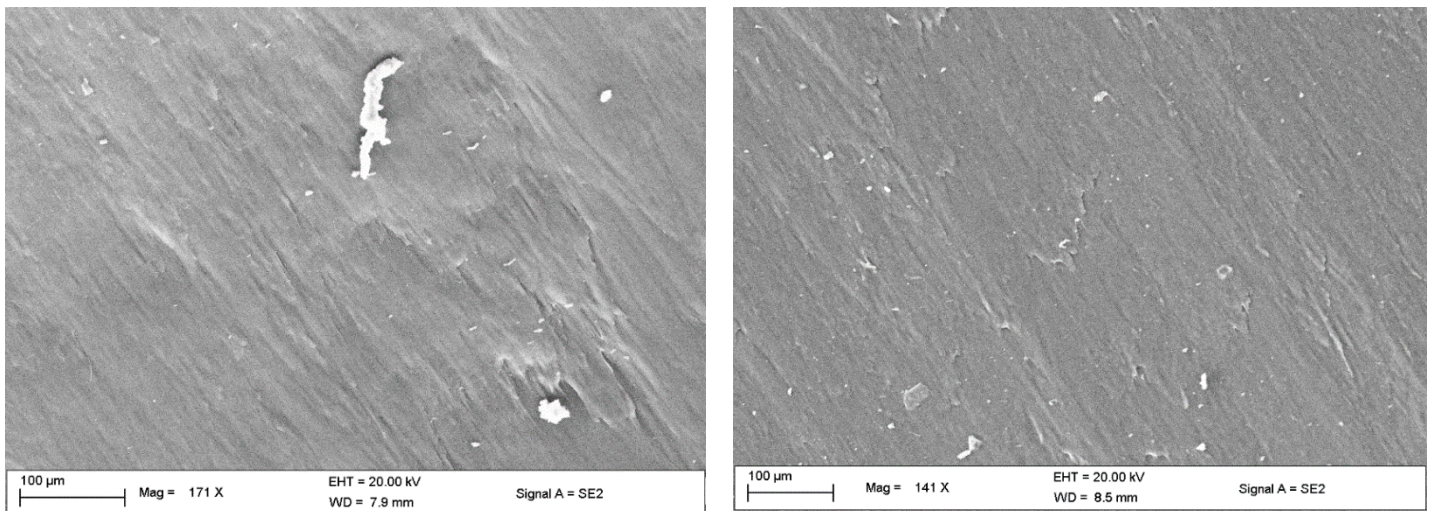
Figure 4.4: SEM Images Showing the Surface Topography of Unmodified Polypropylene.

Table 4.4: EDX results for Unmodified Polypropylene Surface Compositions

Unmodified	Wt%	Wt% Sigma
C	100.00	0.00
Total	100.00	

Figure 4.5 shows the extent of deposition of silica nanoparticles on different areas of the sample. From this image, we can confirm that silica nanoparticles did indeed coat the packing and that the deposition and coating process was non-uniform. The Energy dispersive X-ray (EDX) spectroscopy results in table 4.45 indicates the composition of silica is 4.34 % by mass on the modified Raschig rings. The SEM images also validate the method adapted and applied from Ahsani et al (2015) which was initially intended to modify a polypropylene membrane and not solid packing material. After being able to see the actual deposition of silica nanoparticles on the surface of the polypropylene Raschig ring it can be confirmed that the addition of a chemical structure onto the surface of the polymeric

material increased the hydrophilicity of the polymeric material and improved the wetting and efficiency. It would be interesting to investigate the life span of the added particles; however, this is out of the scope of this investigation.
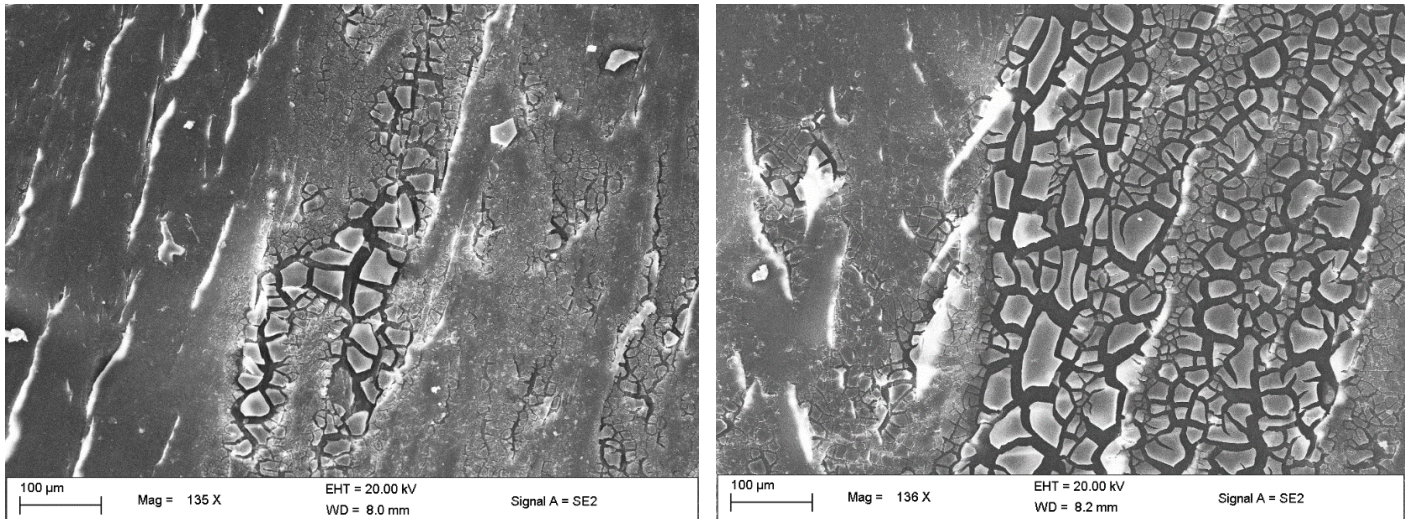
Figure 4.5: SEM Images Showing the Extent of Silica Deposition on the Modified Polypropylene Surface.

Table 4.5: EDX results for Modified Polypropylene Surface Compositions.

Modified	Wt%	Wt% Sigma
C	76.76	0.65
O	18.90	0.66
Si	4.34	0.13
Total	100.00	

4.2 Part B – Absorption Performance

This investigation is the follow-up from part A in which the modified polypropylene packing was created and the wetting efficiency of the different packing types were investigated. To test the performance of the modified polypropylene packing, the existing setup was modified to an absorption column. An inlet gas line was connected to the bottom of the existing glass column next to the exit

liquid line. The gas selected for the investigation was carbon dioxide while the liquid was water. This system was selected as it is simple, non-toxic and performance can be measured using the titration method. A carbon dioxide cylinder was connected to a rotameter which had to be calibrated while the water was pumped from a tank into the top of the column using a peristaltic pump. This pump was selected due to its 'contamination-free' operation. The fluid being pumped is confined to the tubing so the pump does not contaminate the fluid and the fluid does not foul the pump. Peristaltic pumps are also non-siphoning which prevents back flow of fluid and promotes accurate and steady dispensing into the column. The titration method involved the exit liquid line being transferred into a stirred beaker containing sodium hydroxide. The absorbed carbon dioxide would then react with the sodium hydroxide to produce sodium carbonate and water. A 100 mL sample of the solution would then be titrated with hydrochloric acid to attain a pH curve. Different molar concentrations of the sodium hydroxide and hydrochloric acid solutions were used for this experiment.

For set 1 of the experiment, it was decided to keep the water flow constant at the lowest setting on the pump which was 122 mL/min. The gas entering the column was pure carbon dioxide and was varied for each run as can be seen in table 4.6 below. The sodium hydroxide and hydrochloric acid solutions were chosen to be 0.1 M for this set of runs. The glass, unmodified and modified packing were used for this run and the packing height was selected to be 280 mm. The results for set 1 can be seen in figure 4.6 while the percentage improvement of the modified packing when compared to the unmodified packing can be seen in figure 4.7 below.

Table 4.6: Carbon dioxide flowrates for Set 1.

Carbon dioxide flowrates (cm^3/min)	25.38	52.52	74.07	90.98

Figure 4.6: Carbon dioxide absorbed vs L/G ratio results for Set 1.
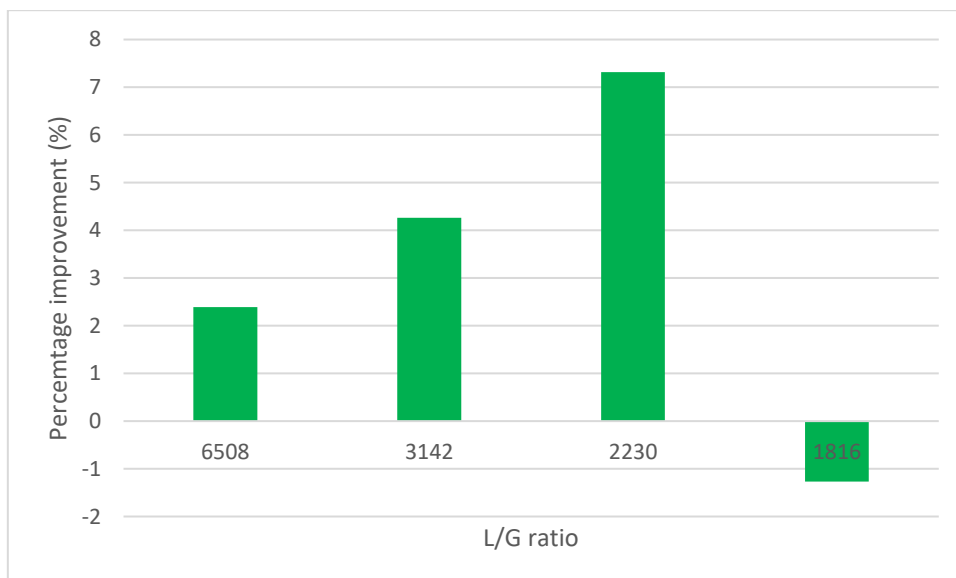
Figure 4.7: Percentage improvement of modified packing to unmodified packing for Set 1.

The results above show that the modified packing performed better than the unmodified packing for the three higher L/G ratios and slightly worse for the lowest ratio. The difference in carbon dioxide absorbed by the different packing were minimal as almost all the carbon dioxide entering the column was being absorbed. The high driving force for mass transfer as the gas is pure carbon dioxide and the concentration in liquid phase is low. This results in high mass transfer rates and good performance for the absorption regardless of column wetting and packing type. Some modifications were needed to be made to get a more clearer and accurate result when comparing the three types of packing. For set 2 of the experiment, some modifications had to be made as the column performance was very high

for set 1. The first change made was the packed height of the column, it was reduced from 280 mm to 90 mm. This would allow less contact time between the gas and the liquid and show which packing is performing better in each case. The second change involved diluting the carbon dioxide concentration in the gas stream. An inert gas needed to be added to the stream and used in the correct ratios to dilute the carbon dioxide. The inert gas chosen to be used was nitrogen and was connected to a rotameter for flow control. The total flowrate for the gas was kept to approximately 120 cm^3/min. The results for set 2 can be seen in figure 4.8 while the percentage improvement of the modified packing when compared to the unmodified packing can be seen in figure 4.9 below.

Figure 4.8: Carbon dioxide absorbed vs concentration of carbon dioxide results for Set 2.
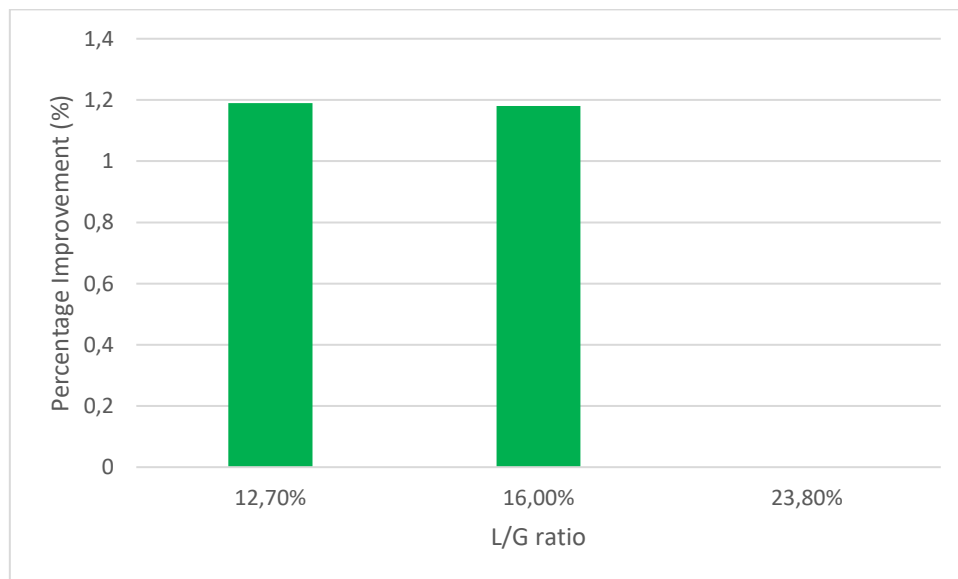
Figure 4.9: Percentage improvement of modified packing to unmodified packing for Set 2.

The results above show that the modified packing is performing at a higher level than the glass and unmodified packing. At 12.70 % and 16.00 % concentration of carbon dioxide, the improvement of the modified to unmodified can be seen clearly in figure 4.8. The lower concentrations of carbon dioxide made it more difficult to be absorbed enabling the results to show which packing performed the best. It can be seen that as you increase the concentration of CO2 you increase the driving force for mass transfer and hence the amount of CO2 absorbed increases. The modification made helped improve the results obtained but more changes needed to be made. The inlet of the gas line entered at the bottom of the column where the exit liquid line was. It could be seen that the outlet liquid would accumulate and the entering gas would come into immediate contact with that liquid before moving through the packed column. The carbon dioxide being absorbed in that initial contact would increase the amount absorbed by each packing even though the packing was not involved. To overcome this problem, the packing had to be raised by attaching a metal stand to the bottom of the column which raised the packing 50 mm from the bottom of the column. A metal tube was attached to the gas inlet of the column which ensured that the gas entering the column was not in contact with the accumulating liquid in the bottom of the column and only in contact with the liquid in the packed column. The carbon dioxide concentration was kept at a constant 16 % for set 3 while the liquid flow varied as can be seen table 4.7 and the packing height was 280 mm. The flowrate for the gas was kept to approximately 120 cm^3/min. The hydrochloric and sodium hydroxide solutions were changed to 0.01 M and 0.02 M respectively to acquire more accurate inflection points in the titration curve. The results for set 3 can be seen in figure 4.10 while the percentage improvement of the modified packing when compared to the unmodified packing can be seen in figure 4.11 below.

Table 4.7: Liquid flowrates for Set 3.

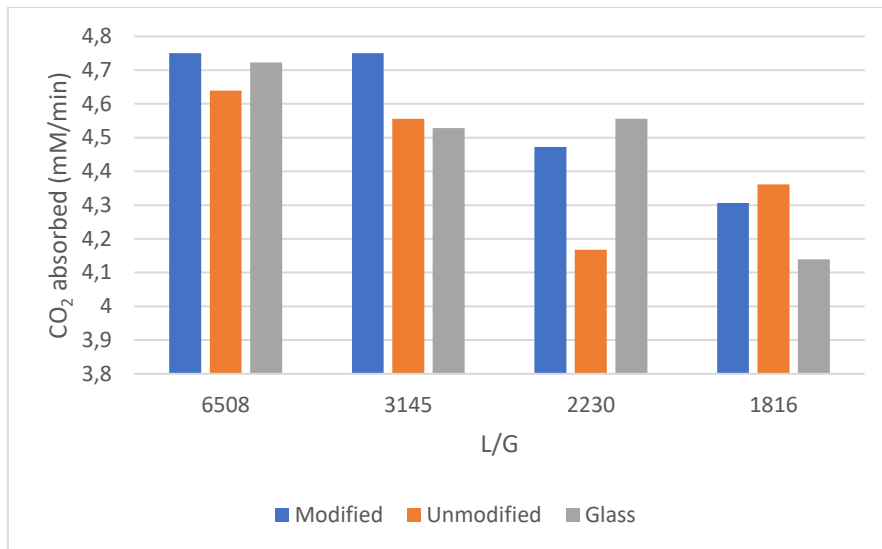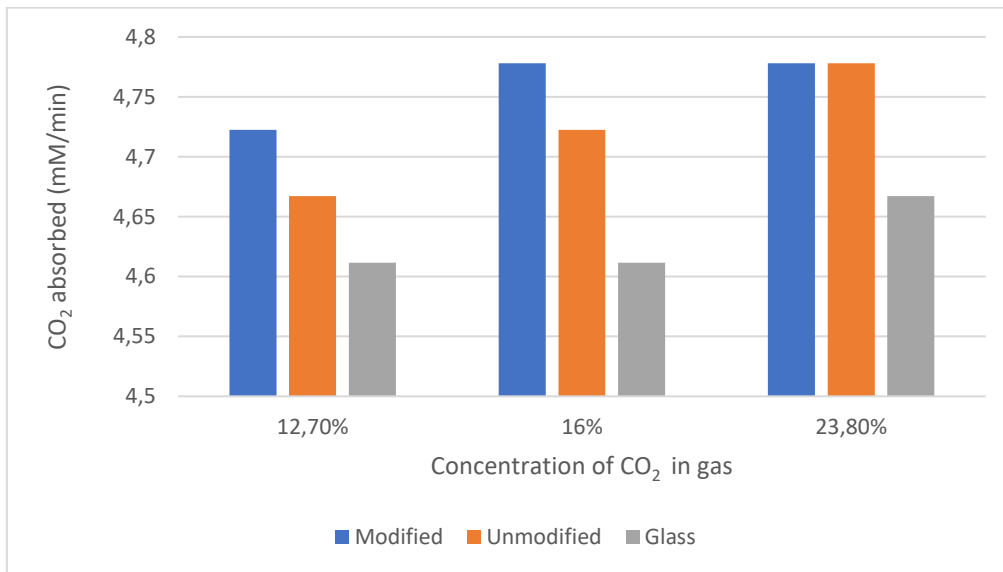| Liquid flowrates (mL/min)	122	390	555

Figure 4.10: Carbon dioxide absorbed vs L/G ratio results for Set 3.
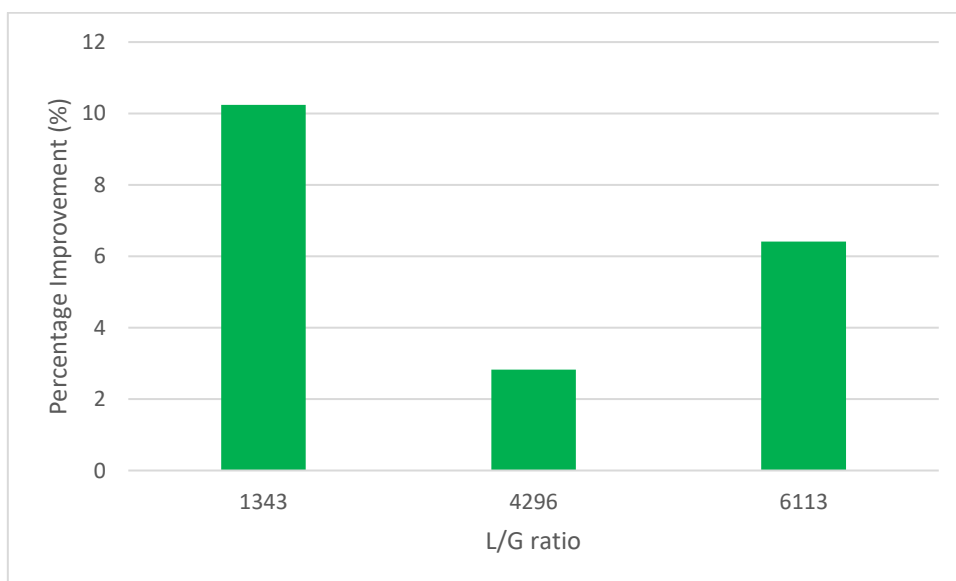
Figure 4.11: Percentage improvement of modified packing to unmodified packing for Set 3.

The new molar concentrations of hydrochloric acid and sodium hydroxide have given more accurate inflection points on the titration curve. The inflection points are vital in the calculation approach for determining the amount of carbon dioxide being absorbed. Varying the liquid flowrates varies the L/G ratio and shows performance of the packing at different liquid flows. The lowest liquid flowrate of 122 mL/min produced a L/G ratio of 1343 and the modified packing performed better than the glass and 10.24 % better than the unmodified packing in this condition. The modified performed best with the L/G ratio of 6113 and second best to glass for the L/G ratio of 4296. Further increases beyond a 4000-

5000 L/G ratio will have little effect on the overall absorption of CO2 as possible a limiting value has been reached. To examine the performance of the different packings in more detail, the column height was changed back to 90 mm and the other variables were left unchanged for set 4. The results for set 4 can be seen in figure 4.12 while the percentage improvement of the modified packing when compared to the unmodified packing can be seen in figure 4.13 below.

Figure 4.12: Carbon dioxide absorbed vs L/G ratio results for Set 4.

Figure 4.13: Percentage improvement of modified packing to unmodified packing for Set 4.

The decrease in column height is to investigate the performance of the different packing with less amount of surface area for absorption. The modified packing produced the best results with it absorbing the highest amount of carbon dioxide in all 3 runs for set 4. The percentage improvement of the modified packing to the unmodified was clearly visible here with the highest improvement being 9.36% for the L/G ratio of 1343.

For low concentrations of carbon dioxide, the titration method would not be very accurate and the gas analyser was used to indicate the carbon dioxide concentration in the gas inlet and outlet with the difference between that being the amount of carbon dioxide absorbed. The packed height for set 5 was kept at 90 mm with three liquid flowrates also being kept the same. The concentration of carbon dioxide was set at 0.683 %. The total gas flowrate was kept to approximately 120 cm^3/min so the L/G ratios are similar to previous sets of results. The results for set 5 can be seen in figure 4.14 while the percentage improvement of the modified packing when compared to the unmodified packing can be seen in figure 4.15 below.
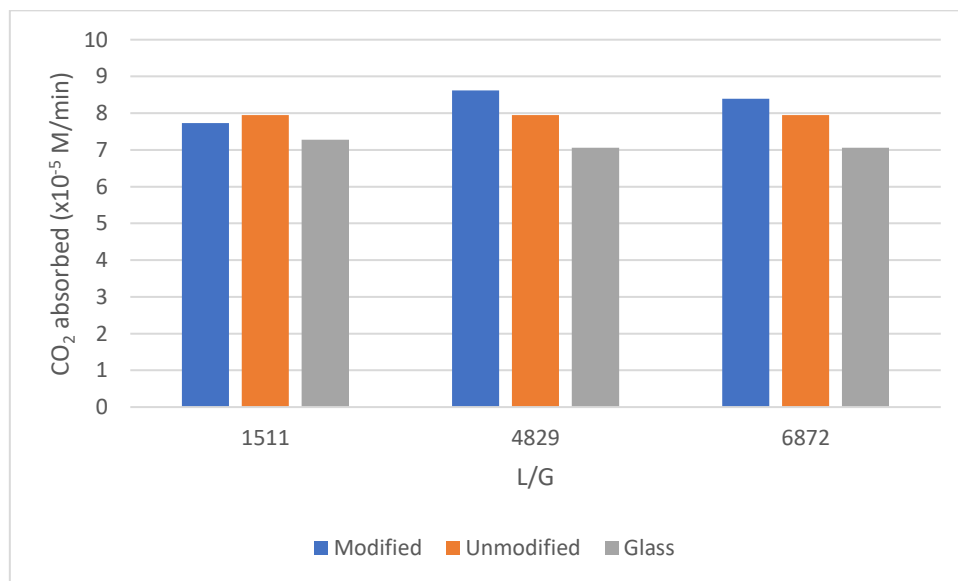
Figure 4.14: Carbon dioxide absorbed vs L/G ratio results for Set 5.
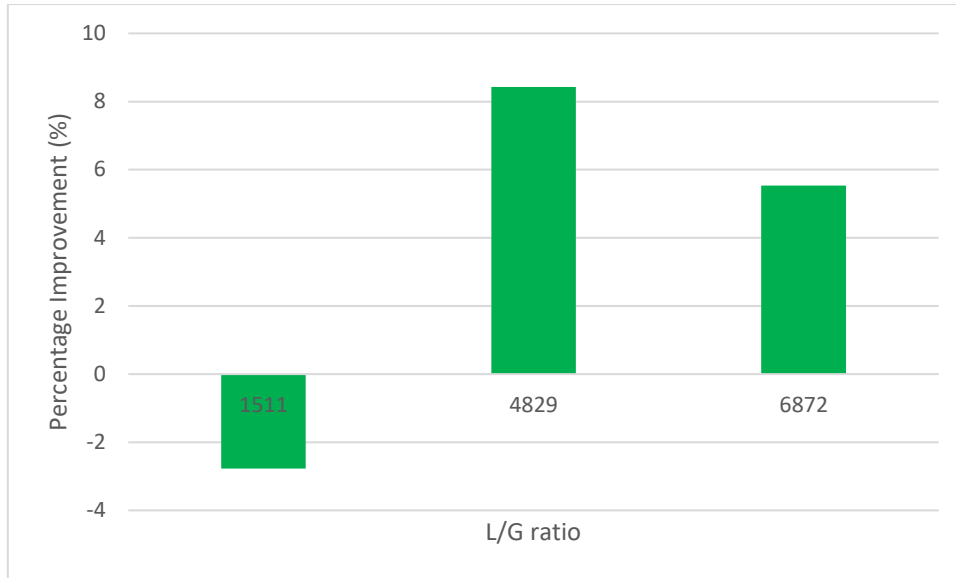
Figure 4.15: Percentage improvement of modified packing to unmodified packing for Set 5.

The modified packing was once again superior with medium and high L/G ratios with an 8.43 % and 5.53 % improvement to the unmodified packing. The low L/G ratio showed similar amounts of carbon dioxide being absorbed for the three packing with the modified being slightly better than the glass but 2.77 % worse off than the unmodified. This may be due to poor liquid distribution in the column at this lower flowrate. At a lower liquid flowrate, the water has less time to distribute around the liquid distribution cap at the top of the column whereas at higher water flowrates water is allowed to build up at the top of the column before being distributed. The low concentration of carbon dioxide in the gas stream needs a better liquid distribution in the column to ensure optimum absorption. For set 6 of the experiment, the carbon dioxide concentration was changed to 2.167 % while keeping the total gas flowrate to approximately 120 cm^3/min. The results for set 6 can be seen in figure 4.16 while the percentage improvement of the modified packing when compared to the unmodified packing can be seen in figure 4.17 below.
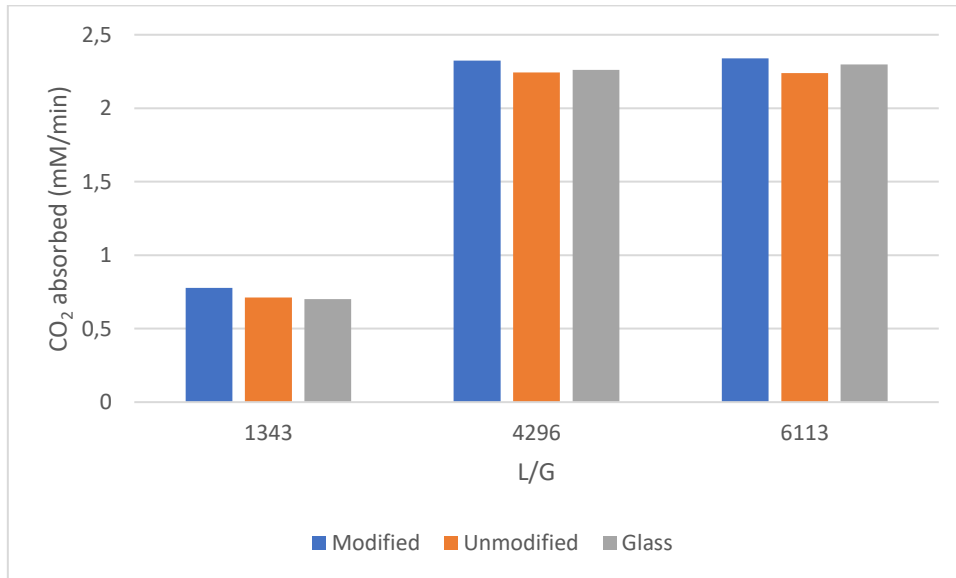
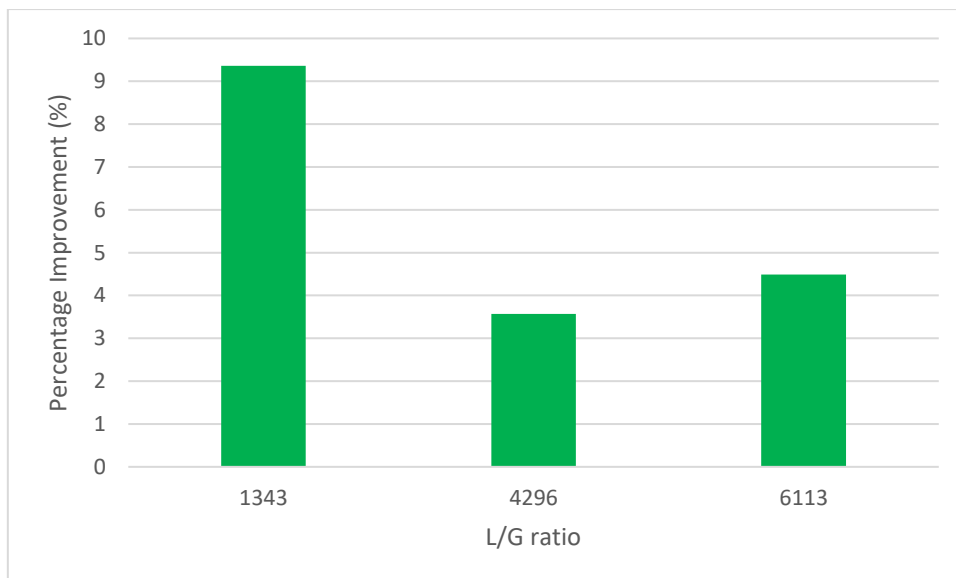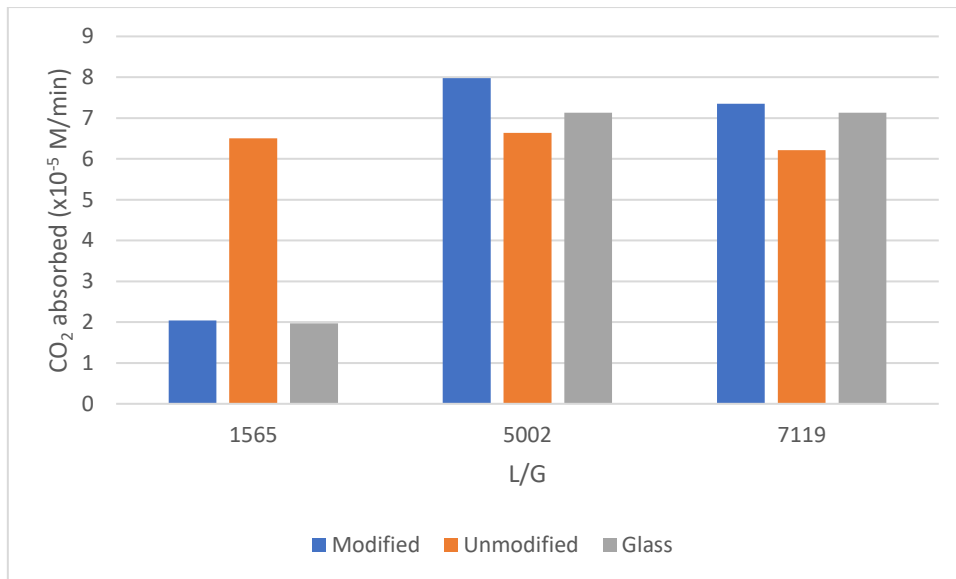*Figure 4.16: Carbon dioxide absorbed vs L/G ratio results for Set 6.*
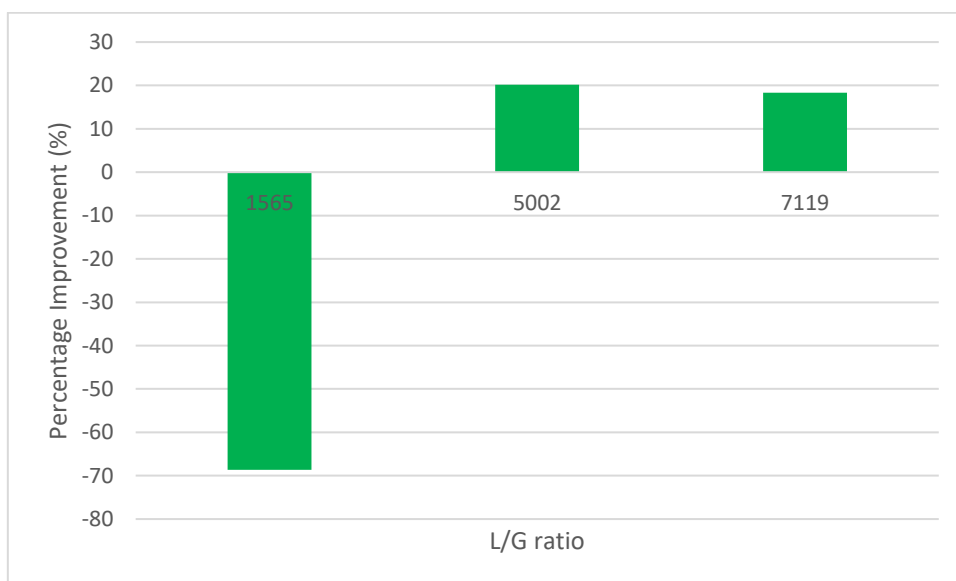
Figure 4.17: Percentage improvement of modified packing to unmodified packing for Set 6.

The modified packing was once again superior with medium and high L/G ratios with a 20.18 % and 18.36 % improvement to the unmodified packing. The low L/G ratio showed similar amounts of carbon dioxide being absorbed for the modified and the glass but a much higher amount being absorbed for the unmodified. The amount of carbon dioxide absorbed for the L/G ratio of 1565 in the unmodified packed column is abnormally high. This may have been due to malfunction of the gas analyser or abnormal liquid distribution in the column. Unfortunately, the analyser thereafter required servicing

and repeat measurements at this L/G ratio could not be carried out. The gas analyser method showed similar trends to previous results for the modified packing as it performed the best for absorption in the medium and high L/G ratios.

Overall it can be deduced that the modified packing had performed the best among the three packings. The glass packing was smaller in size than the modified and unmodified packing. The smaller packing means that more of the glass Raschig rings were used in the column to obtain the same packing height. The increased number of glass Raschig rings would increase the total surface area for contact between the gas and liquid phases in the column. The glass packing should therefore have better absorption due to its increased contact area. The fact that the modified packing is performing better even with the lower surface area, shows that the modification with the silica nanoparticles has definitely improved wetting efficiency. The modified packing also performed better than the unmodified packing in most of runs, this shows us that modifying the polypropylene packing has improved the overall performance of the packing.

CHAPTER 5: CONCLUSIONS

The stimulus response technique based on the tracer method is a successful method when determining the RTD and estimating the wetting efficiency for the different packing materials. The modified polypropylene Raschig rings was found to have the highest mean residence time and wetting efficiency. It was found that unmodified polypropylene Raschig rings had a higher wetting efficiency than the glass although having the same mean residence time. From contact angle measurement, it can be deduced that modification by coating with silica nanoparticles increased the hydrophilicity of the polymeric material. Hence, an increase in wettability and wetting efficiency of polypropylene was brought about. SEM images showed that silica nanoparticles were definitely present on the polypropylene surface and that the extent of deposition was non-uniform.

A 50 mm inner diameter glass column, with fittings to work as an absorber was packed to a different heights with glass, unmodified or modified polypropylene Raschig rings for each run. The titration method was successful for analysis on the amount of carbon dioxide being absorbed per a run. The two inflection points were found to be in the desired range in each run. The 0.1 M solutions of sodium hydroxide and hydrochloric acid used in set 1 and 2 of the absorption performance runs results were found to be too strong of a solution to enabled us to better distinguish between the amounts of CO_2 absorbed by the different packings. The 0.02 M sodium hydroxide and 0.01 M hydrochloric acid solutions used in set 3 and 4 of the absorption performance runs obtained more accurate inflection points and hence more accurate results for carbon dioxide being absorbed. Pure carbon dioxide used as the gas inlet produced almost perfect absorption for all packing and therefore a more dilute mixture had to be used. The liquid flowrates of 390 and 555 mL/min produced similar results indicating that higher liquid flowrates will not substantially increase the amount of carbon dioxide being absorbed. The higher the liquid flow, the more contact there is between the gas and liquid which therefore increases the amount of carbon dioxide being absorbed. The modified polypropylene packing performed the best during most of runs and verified it having the highest wetting efficiency and mean resistance time. For the 280 mm and 90 mm packed height with a 16 % carbon dioxide inlet concentration, modified packing showed improvements on absorption for all liquid flowrates for up to 10.24 % and 9 36% respectively when compared to the unmodified packing. The glass and unmodified packing performance varied with different factors. At a lower L/G ratios, the unmodified and glass packing performance were very similar while at medium and higher L/G ratios the glass packing performed better. The modified packing when compared to the unmodified packing

performed at a superior level which indicates that the silica nanoparticle modifications were successful on direct application within a packed absorber column.

The gas analyser method produced viable results for the lower concentrations of carbon dioxide with the medium and high liquid flowrates. The low liquid flowrate results were not conclusive. At a lower liquid flowrate, the water had less time to distribute around the liquid distribution cap at the top of the column whereas at higher water flowrates water can build up at the top of the column before being distributed. With the concentration of carbon dioxide being low for these runs, the better the liquid distribution, the more area there is for the gas to contact the liquid and allow for absorption. The modified packing absorption performance was superior to the glass and unmodified packing at the medium and high liquid flowrates. With a packed height of 90 mm and inlet carbon dioxide concentration of 0.683 %, the modified packing showed improvements on absorption for the medium and high liquid flowrates at 8.43 % and 5.53 % respectively when compared to the unmodified packing. At an inlet carbon dioxide concentration of 2.167 %, the improvements were 20.18 % at the medium liquid flowrate and 18.36 for the high liquid flowrate. The amount of carbon dioxide being absorbed increased as the L/G ratios increased. It was found that increasing beyond a 4000-5000 L/G ratio will have little effect on the overall absorption of carbon dioxide as possibly a limiting value has been reached.

The overall investigation was a success in showing that the modified polypropylene packing was superior to the unmodified and glass packing in using wetting efficiency and mean residence time experiments. The absorption performance part of the investigation verifies that the modified packing outperformed the glass and unmodified packing in application while varying gas and liquid flowrates, gas compositions and packed height. The modified packing shows potential of commercialisation and application on an industrial level as it is cost effective and shows an improved performance to the unmodified packing particularly for aqueous systems.

REFERENCES

1. Ahsani, M. & Yegani, R., 2015. Study on the fouling behaviour of silica nanocomposite modified polypropylene …. *Chemical Engineering Research and Design,* Issue 2, pp. 261-273.

2. Ataki, A., 2006. *Wetting of Structured Packing Elements - CFD and Experiment ,* Kaiserslautern: s.n.

3. Athauda, T.J. et al., Materials Letters (2012) 67, pp. 338-341.

4. Azmi, M. I., 2013. *Measurement of Wetting Efficiency in Packed Tower Using Stimulus Response Technique. ,* Perak: s.n

5. Elements, N. I., n.d. *NIS Elements Viewer- Interactive Measurement.* s.l.:Nikon

6. Fang, J. et al., Journal of Materials Chemistry (2010) 20, pp. 1651-1653.

7. Fogler, H. S., 1999. *Elements of Chemical Reaction Engineering.* 3rd ed. New Delhi: Prentice-Hall.

8. Hwang, J. and Ahn, Y., Bulletin of the Korean Chemical Society (2015) 36, pp. 391-394.

9. Ibrahim, I. A., Zikry, A. A. & Sharaf, M. A., 2010. Preparation of Spherical Silica Nanoparticles: Stober Silica. *Journal of American Science,* 6(11).

10. Julcour-Lebigue, C., Baussaron, L., Delmas, H. & Wilhelm, A.-M., 2007. Theoretical Analysis of Tracer Method for the Measurement of Wetting Efficiency. *Chemical Engineering Science,* Issue 62, pp. 5374-5379.

11. Ke, Q. et al., Surface and Coatings Technology (2011) 205, pp. 4910-4914.

12. Krell, E., 1982. In: *Handbookof Laboratory Distillation.* Amsterdam: Elsevier, pp. 49-53.

13. Levenspiel, O., 1999. *Chemical Reaction Engineering.* 3rd ed. New York: John Wiley & Sons, Inc.

14. Ponter, A.B. et al., Chemical Engineering Technology (1976) 48, pp. 635-636.

15. Rase, H.F., 1977. *Chemical Reactor Design for Process Plants.* Vol 1. New York: John Wiley & Sons, Inc.

16. Saeed, S. et al., 2015. Comparison and Modeling of Various Packing Materials in a Packed Column Using Two Slightly Soluble Solute Gases. *International Journal of Innovation and Scientific Research,* 17(1), pp. 186-190.

17. Seader, J. D. & Henley, E. J., 2006. *Separation Process Principles.* 2nd ed. New Jersey: John Wiley & Sons, Inc.

18. Yuan, Y. H. & Lee, T. R., 2013. Contact Angle and Wetting Properties. In: *Surface Science Tecchniques.* Berlin; New York: Springer.

APPENDIX A: RAW DATA

A.1. Part A - Determination of wetting efficiency of polymeric packing

Table A-1: Raw Data for Glass Raschig Rings in RTD experiment.

	Run 1	Run 2	Run 3
Time (s)	Conductivity (µS/cm)	Conductivity (µS/cm)	Conductivity (µS/cm)
0	0.33	0.33	0.33
3	12.6	12.6	1.43
6	1321	1317.9	12.6
9	8680	9100	1314
12	2960	4750	7800
15	1261	1534	4240
18	297	427	1326
21	120	204	522.1
24	58.7	120	175
27	30.8	44.6	81.3
30	22.1	26.3	41.2
33	14.25	16.9	26.27
36	12.08	14.33	18.79
39	7.62	12.7	12.9
42	6.36	7.78	8.7
45	4.85	6.9	8.04
48	3.79	6.64	6.73
51	3.47	6.94	4.99
54	2.97	4.36	4.51
57	2.7	3.75	4.43

60	2.04	3.67	3.71
63	1.94	3.7	3.34
66	1.58	3.77	3.2
69	2.13	2.93	2.95
72	2.08	2.29	3.02
75	2.79	2.1	2.44
78	2.56	2.32	2.7
81	2.15	1.83	2.43
84	1.55	2.03	2.14
87	1.48	1.65	2.02
90	1.17	1.55	1.95
93	1.79	1.76	1.58
96	1.45	1.54	1.37
99	1.1	1.27	1.22
102	1	1.09	1.48
105	0.91	1.01	1.49
108	1.04	1.94	1.43
111	0.83	1.85	1.2
114	0.97	1.98	1.14
117	0.99	1.37	1.13
120	0.81	1.16	1.07
123	0.8	0.95	1.12
126	0.93	0.87	1.02
129	0.85	1.06	0.92
132	0.66	2.41	0.92
135	0.73	2.32	0.86

138	0.7	2.8	0.87
141	0.69	2.24	1.03
144	0.74	1.86	1.12
147	0.68	1.33	1.11
150	0.6	1.11	1.24
153	0.6	1.21	1.02
156	0.62	0.87	0.97
159	0.7	0.91	0.77
162	0.63	0.78	0.74
165	0.64	0.98	1.02
168	0.59	1.03	0.76
171	0.59	0.81	0.76
174	0.63	0.71	0.77
177	0.59	0.76	0.75
180	0.59	0.73	0.7
183	0.5	0.66	0.71
186	0.49	0.7	0.71
189	0.51	0.67	0.69

192	0.61	0.58	0.69
195	0.56	0.59	0.68
198	0.54	0.58	0.68
201	0.52	0.49	0.61
204	0.6	0.51	0.55
207	0.49	0.59	0.7
210	0.55	0.56	0.67

213	0.51	0.54	0.62
216	0.53	0.59	0.5
219	0.51	0.56	0.61
222	0.5	0.54	0.54
225	0.49	0.53	0.55
228	0.48	0.45	0.6
231	0.52	0.52	0.49
234	0.5	0.76	0.58
237	0.51	0.64	0.58
240	0.42	0.47	0.49

Table A-2: Raw Data for Unmodified Polypropylene Raschig Rings.

	Run 1	Run 2	Run 3
Time (s)	Conductivity (µS/cm)	Conductivity (µS/cm)	Conductivity (µS/cm)
0	0.33	0.33	0.33
3	5.72	13.1	6.28
6	1364	1362	130.7
9	4890	5000	5220
12	2450	3090	2630
15	1301	1301	2430
18	130.8	233	1300
21	230	124.5	556
24	124.6	42.8	337
27	110	32.4	124.4
30	98.3	22.3	92.3

33	93.4	16.17	58.6
36	34.8	8.45	36.2
39	34.3	13.1	26
42	17.57	19.81	12.45
45	12.46	4.72	12.32
48	14.64	2.94	9.89
51	7.15	4.8	10.75
54	13.11	3	5.62
57	5.78	2.62	2.81
60	8.11	5.11	2.82
63	6.26	2.19	1.81
66	9.81	2.72	1.35
69	8.16	3.73	2.2
72	2.64	10.94	1.17
75	3.03	5.07	2.41
78	8.16	2.03	1.13
81	12.46	1.88	4.61
84	2.28	2.51	1.5

87	10.49	1.07	1.83
90	1.42	0.81	1.01
93	3.84	0.93	0.85
96	2.42	0.96	2.03
99	1.45	1.82	2.59
102	3.41	1.97	2.62
105	2.55	1.31	1.91

108	1.74	0.97	1.83
111	2.01	0.88	0.66
114	0.81	0.89	0.69
117	0.71	0.71	0.64
120	0.62	0.65	0.66
123	0.6	0.51	0.7
126	1.01	0.89	0.67
129	0.69	0.69	0.6
132	0.66	7.2	0.5

Table A-3: Raw Data for Modified Polypropylene Raschig Rings.

	Run 1	Run 2	Run 3
Time (s)	Conductivity (µS/cm)	Conductivity (µS/cm)	Conductivity (µS/cm)
0	0.33	0.33	0.33
3	4.94	4.62	6.68
6	85.3	80.3	88.3
9	1360	1338	1463
12	5260	2800	4280
15	4230	5648	5001
18	3489	4270	4896
21	2675	3569	3564
24	1030	2897	2490
27	206	1023	1569
30	195.3	586	523

33	125.6	468	312
36	85.2	264	229
39	58.6	140.5	157
42	41.9	70.4	124.2
45	24.4	50.3	56.25
48	15.74	34.2	33.1
51	195.3	23.4	22.36
54	125.6	17.63	17.82
57	85.2	14.43	14.39
60	58.6	13.08	13.43
63	41.9	12.32	13.11
66	24.4	12.43	13.08
69	15.74	8.46	12.43
72	12.43	7.17	5.76
75	12.54	6.05	3.56
78	12.43	5.91	2.74
81	10.56	6.82	2.73
84	9.2	6.68	2.68
87	8.42	5.16	2.67
90	8.2	2.82	1.84
93	8.02	2.79	1.38

96	5.62	2.26	1.58
99	2.57	1.51	1.49
102	1.54	1.79	0.84
105	1.12	0.57	1.15

108	2.62	0.61	1.65
111	3.4	0.69	0.96
114	2.03	1.53	0.84
117	1.07	0.81	1.15
120	3.67	0.51	1.65
123	2.34	1.39	0.96
126	2.04	0.59	0.74
129	1.48	1.44	1.33
132	2.48	0.35	0.73
135	1.89	1.81	0.75
138	4.55	1.24	0.63
141	1.84	0.63	0.99
144	1.75	0.53	0.75
147	1.84	0.52	0.54
150	1.61	0.69	0.61
153	1.71	0.68	0.59
156	1.74	0.52	0.58
159	1.68	0.5	0.49
162	1.54	0.48	0.44
165	1.52	0.47	0.45
168	1.48	0.44	0.45
171	1.2	0.45	0.44
174	1	0.44	0.45
177	1.1	0.43	0.44
180	1.08	0.42	0.43
183	1.07	0.42	0.43

A.2. Part B – Absorption Performance

Table A-4: Raw Data for Glass Raschig Rings of Titration Method for Set 1.

Glass Packing							
0,1 M NaOH and 0,1 M HCl + Liq flow of 122 mL/min							
28 cm Packed Height							
100 % CO2							
Gas flow - 25,38		Gas flow - 52,52		Gas flow - 74,07		Gas flow - 90,98	
Run 2		Run 3		Run 1		Run 4	
Vol(cm3)	pH	Vol(cm3)	pH	Vol(cm3)	pH	Vol(cm3)	pH
0	12,24	0	12,21	0	12,18	0	12,12
2	12,21	2	12,2	2	12,16	2	12,09
4	12,19	4	12,18	4	12,15	4	12,07
6	12,17	6	12,16	6	12,13	6	12,03
8	12,14	8	12,13	8	12,1	8	12
10	12,11	10	12,1	10	12,07	10	11,96
12	12,08	12	12,06	12	12,03	12	11,91
14	12,05	14	12,03	14	12	14	11,87
16	12,01	16	11,99	16	11,96	16	11,81
18	11,97	18	11,95	18	11,92	18	11,75
20	11,92	20	11,91	20	11,88	20	11,67
22	11,88	22	11,86	22	11,83	22	11,59
24	11,82	24	11,81	24	11,78	24	11,48
26	11,77	26	11,75	26	11,71	26	11,36
28	11,7	28	11,68	28	11,63	28	11,2

30	11,62	30	11,6	30	11,55	30	10,96
32	11,53	32	11,5	32	11,44	32	10,63
34	11,43	34	11,38	34	11,31	32,5	10,53
36	11,28	36	11,22	36	11,13	33	10,44
38	11,06	38	10,99	38	10,85	33,5	10,33
40	10,7	40	10,64	38,5	10,76	34	10,24
40,5	10,58	40,5	10,53	39	10,64	34,5	10,15
41	10,42	41	10,4	39,5	10,52	35	10,05
41,5	10,23	41,5	10,24	40	10,4	35,5	9,96
42	10,01	42	10,1	40,5	10,26	36	9,87
42,5	9,78	42,5	9,95	41	10,12	36,5	9,76
43	9,5	43	9,79	41,5	9,99	37	9,64
43,5	9,12	43,5	9,6	42	9,84	37,5	9,51
44	7,86	44	9,4	42,5	9,69	38	9,37
44,5	7,2	44,5	9,08	43	9,5	38,5	9,22
45	6,71	45	8,29	43,5	9,26	39	8,96
45,5	6,22	45,5	7,37	44	8,94	39,5	8,53
46	5,76	46	6,98	44,5	8,01	40	7,64
46,5	5,01	46,5	6,68	45	7,37	40,5	7,25
47	3,56	47	6,45	45,5	7,06	41	7
47,5	3,18	47,5	6,25	46	6,78	41,5	6,8
48	2,98	48	6,04	46,5	6,53	42	6,65
50	2,61	48,5	5,8	47	6,3	42,5	6,52
52	2,42	49	5,52	47,5	6,07	43	6,41
54	2,29	49,5	5,02	48	5,85	43,5	6,3

56	2,2	50	3,68	48,5	5,59	44	6,2
58	2,11	50,5	3,23	49	5,17	44,5	6,09
60	2,05	51	3,02	49,5	4,01	45	5,96
62	2	51,5	2,88	50	3,34	45,5	5,84
64	1,95	52	2,77	50,5	3,09	46	5,7
66	1,91		2,51	51	2,93	46,5	5,53
68	1,87		2,34	53	2,61	47	5,28
			2,23	55	2,42	47,5	4,81
			2,15	57	2,29	48	3,66
			2,07	59	2,19	48,5	3,2
			2,01	61	2,11	49	2,99
			1,96	63	2,05	51	2,6
			1,91	65	2	53	2,4
				67	1,95	55	2,27
				69	1,91	57	2,17
						59	2,09
						61	2,02
						63	1,96
						65	1,92

Unmodified Packing							
0,1 M NaOH and 0,1 M HCl + Liq flow of 122 mL/min							
28 cm Packed Height							
100 % CO2							
Gas flow - 25,38		Gas flow - 52,52		Gas flow - 74,07		Gas flow - 90,98	
Run 5		Run 7		Run 8		Run 6	
Vol(cm3)	pH	Vol(cm3)	pH	Vol(cm3)	pH	Vol(cm3)	pH
0	12,41	0	12,34	0	12,32	0	12,32
2	12,39	2	12,32	2	12,29	2	12,3
4	12,36	4	12,29	4	12,25	4	12,27
6	12,32	6	12,26	6	12,22	6	12,23
8	12,29	8	12,22	8	12,18	8	12,2
10	12,24	10	12,19	10	12,13	10	12,17
12	12,2	12	12,15	12	12,09	12	12,13
14	12,15	14	12,11	14	12,04	14	12,09
16	12,1	16	12,07	18	11,94	16	12,05
18	12,05	18	12,02	20	11,86	18	11,99
20	11,99	20	11,96	22	11,78	20	11,94
22	11,92	22	11,9	24	11,7	22	11,88
24	11,85	24	11,84	26	11,58	24	11,82
26	11,76	26	11,77	28	11,42	26	11,74
28	11,6	28	11,69	30	11,2	28	11,66

30	11,52	30	11,58	32	10,9	30	11,55
32	11,35	32	11,47	34	10,5	32	11,42
34	11,11	34	11,29	34,5	10,4	34	11,24
36	10,67	36	11,06	35	10,28	36	10,99
38	9,98	38	10,68	35,5	10,16	38	10,59
38,5	9,79	40	10,07	36	10,08	40	10,11
39	9,47	40,5	9,92	36,5	9,95	40,5	10
39,5	8,8	41	9,71	37	9,83	41	9,84
40	7,68	41,5	9,48	37,5	9,67	41,5	9,69
40,5	7,27	42	9,21	38	9,49	42	9,52
41	6,94	42,5	8,69	38,5	9,27	42,5	9,33
41,5	6,66	43	7,51	39	8,84	43	9,08
42	6,39	43,5	7,07	39,5	8,05	43,5	8,65
42,5	6,04	44	6,76	40	7,7	44	7,63
43	5,34	44,5	6,44	40,5	7,48	44,5	7,22
43,5	3,86	45	6,2	41	7,31	45	6,99
44	3,49	45,5	5,94	41,5	7,15	45,5	6,82
44,5	3,29	46	5,66	42	7	46	6,66
45	3,15	46,5	5,18	42,5	6,86	46,5	6,48
45,5	3,05	47	3,86	43	6,74	47	6,28
46	2,97	47,5	3,29	43,5	6,61	47,5	6,1
48	2,75	48	3,03	44	6,47	48	5,87
50	2,62	50	2,6	44,5	6,33	48,5	5,64
52	2,52	52	2,4	45	6,18	49	5,31
54	2,44	54	2,27	45,5	5,98	49,5	3,79

56	2,37	56	2,17	46	5,67	50	3,23
58	2,31	58	2,09	46,5	4,93	50,5	3
60	2,26	60	2,02	47	3,84	51	2,84
62	2,22	62	1,97	47,5	3,49	51,5	2,52
64	2,18	64	1,92	48	3,29	52	2,35
66	2,14	66	1,87	48,5	3,15	54	2,23
				49	3,05	56	2,13
				49,5	2,97	58	2,06
				50	2,91	60	1,99
				52	2,73	62	1,94
				54	2,6	64	1,9
				56	2,51		
				58	2,44		
				60	2,37		
				62	2,31		
				64	2,27		
				66	2,23		
				68	2,19		
				70	2,15		

Table A-6: Raw Data for Modified Raschig Rings of Titration Method for Set 1.

Modified Packing							
0,1 M NaOH and 0,1 M HCl + Liq flow of 122 mL/min							
28 cm Packed Height							
100 % CO2							
Gas flow - 25,38		Gas flow - 52,52		Gas flow - 74,07		Gas flow - 90,98	
Run 9		Run 10		Run 11		Run 12	
Vol(cm3)	pH	Vol(cm3)	pH	Vol(cm3)	pH	Vol(cm3)	pH
0	12,45	0	12,22	0	12,39	0	12,21
2	12,42	2	12,19	2	12,36	2	12,2
4	12,39	4	12,17	4	12,33	4	12,17
6	12,36	6	12,15	6	12,3	6	12,14
8	12,32	8	12,13	8	12,26	8	12,11
10	12,29	10	12,09	10	12,23	10	12,07
12	12,25	12	12,07	12	12,19	12	12,04
14	12,22	14	12,03	14	12,15	14	12
16	12,18	16	11,99	16	12,1	16	11,96
18	12,14	18	11,95	18	12,06	18	11,92
20	12,08	20	11,9	20	12	20	11,86
22	12,04	22	11,85	22	11,95	22	11,81
24	11,98	24	11,8	24	11,88	24	11,74
26	11,92	26	11,74	26	11,81	26	11,67
28	11,85	28	11,67	28	11,72	28	11,59
30	11,77	30	11,59	30	11,61	30	11,5
32	11,69	32	11,49	32	11,47	32	11,37

34	11,58	34	11,37	34	11,3	34	11,22
36	11,45	36	11,21	36	11,05	36	11,01
38	11,26	38	10,96	38	10,66	38	10,64
40	10,96	40	10,5	38,5	10,54	38,5	10,51
42	10,4	40,5	10,36	39	10,41	39	10,37
42,5	10,21	41	10,18	39,5	10,27	39,5	10,24
43	10,01	41,5	10	40	10,13	40	10,1
43,5	9,79	42	9,8	40,5	9,98	40,5	9,97
44	9,53	42,5	9,6	41	9,83	41	9,84
44,5	9,13	43	9,28	41,5	9,66	41,5	9,67
45	7,87	43,5	8,67	42	9,45	42	9,49
45,5	7,23	44	7,46	42,5	9,19	42,5	9,27
46	6,79	44,5	6,91	43	8,72	43	8,94
46,5	6,43	45	6,55	43,5	7,63	43,5	8,14
47	6,19	45,5	6,25	44	7,25	44	7,38
47,5	5,84	46	5,96	44,5	6,98	44,5	7,14
48	5,36	46,5	5,63	45	6,76	45	6,93
48,5	3,9	47	5,05	45,5	6,56	45,5	6,74
49	3,31	47,5	3,66	46	6,39	46	6,55
49,5	3,05	48	3,23	46,5	6,27	46,5	6,35
50	2,9	48,5	3,01	47	6,09	47	
52	2,57	49	2,87	47,5	5,86	47,5	6,49
54	2,39	51	2,57	48	5,54	48	6,12
56	2,27	53	2,39	48,5	4,67	48,5	5,61
58	2,18	55	2,27	49	3,47	49	4,06

60	2,1	57	2,18	49,5	3,14	49,5	3,33
62	2,03	59	2,1	50	2,59	50	3,06
64	1,98	61	2,04	52	2,41	50,5	2,9
66	1,94	63	1,99	54	2,28	51	2,78
68	1,9	65	1,94	56	2,18	53	2,51
				58	2,11	55	2,34
				60	2,04	57	2,23
				62	1,98	59	2,14
				64	1,94	61	2,07
						63	2,01
						65	1,96
						67	1,92
						69	1,88

Modified Packing					
0,1 M NaOH + 0,1 M HCl + 9cm packing					
Liq flow - 122 mL/min		Liq flow - 122 mL/min		Liq flow - 122 mL/min	
16% CO2		12,7% CO2		23,8% CO2	
Run 13		Run 14		Run 15	
Vol(cm3)	pH	Vol(cm3)	pH	Vol(cm3)	pH
0	12,63	0	12,54	0	12,66
5	12,55	5	12,46	5	12,59
10	12,47	10	12,37	10	12,51
15	12,37	15	12,26	15	12,42
20	12,26	20	12,13	20	12,31
22	12,21	22	12,07	22	12,26
24	12,15	24	12	24	12,21
26	12,09	26	11,92	26	12,15
28	12,02	28	11,83	28	12,09
30	11,94	30	11,72	30	12,01
32	11,85	32	11,58	32	11,93
34	11,73	34	11,39	34	11,83
36	11,59	36	11,08	36	11,72
38	11,38	38	10,5	38	11,57
40	11,02	38,5	10,31	40	11,34
42	10,29	39	10,08	42	10,9
42,5	10,03	39,5	9,82	42,5	10,69
43	9,71	40	9,45	43	10,46

43,5	9,11	40,5	8,26	43,5	10,13
44	7,72	41	7,39	44	9,72
44,5	7,38	41,5	7,14	44,5	8,14
45	7,07	42	6,93	45	7,27
45,5	6,76	42,5	6,69	45,5	6,82
46	6,28	43	6,33	46	6,21
46,5	4,59	43,5	5,27	46,5	4,49
47	3,66	44	3,66	47	3,67
47,5	3,38	44,5	3,34	47,5	3,39
48	3,23	45	3,16	48	3,24
48,5	3,1	45,5	3,04	48,5	3,12
49	3,01	46	2,94	49	3,03
51	2,78	48	2,71	51	2,79
53	2,64	50	2,57	53	2,66
55	2,54	52	2,47	55	2,56
57	2,47	54	2,39	57	2,48
59	2,4	56	2,32	59	2,42

Table A-8: Raw Data for Unmodified Raschig Rings of Titration Method for Set 2.

Unmodified Packing					
0,1 M NaOH + 0,1 M HCl + 9cm packing					
Liq flow - 122 mL/min		Liq flow - 122 mL/min		Liq flow - 122 mL/min	
16% CO2		12,7% CO2		23,8% CO2	
Run 18		Run 16		Run 17	
Vol(cm3)	pH	Vol(cm3)	pH	Vol(cm3)	pH
Vol(cm3)	pH	Vol(cm3)	pH	Vol(cm3)	pH
0	12,67	0	12,66	0	12,67
5	12,6	5	12,58	5	12,6
10	12,52	10	12,5	10	12,51
15	12,43	15	12,4	15	12,42
20	12,32	20	12,29	20	12,32
22	12,27	22	12,24	22	12,26
24	12,22	24	12,18	24	12,21
26	12,17	26	12,11	26	12,15
28	12,1	28	12,04	28	12,09
30	12,02	30	11,95	30	12,01
32	11,94	32	11,84	32	11,92
34	11,84	34	11,72	34	11,82
36	11,72	36	11,55	36	11,68
38	11,56	38	11,28	38	11,5
40	11,29	40	10,78	40	11,21

42	10,78	40,5	10,58	42	10,61
42,5	10,58	41	10,37	42,5	10,4
43	10,34	41,5	10,14	43	10,2
43,5	10,05	42	9,87	43,5	9,96
44	9,58	42,5	9,49	44	9,66
44,5	8,85	43	8,5	44,5	9,12
45	7,6	43,5	7,56	45	7,76
45,5	7,19	44	7,32	45,5	7,35
46	6,81	44,5	7,11	46	7,09
46,5	6,27	45	6,76	46,5	6,77
47	4,88	45,5	6,2	47	6,32
47,5	3,69	46	4,62	47,5	6,04
48	3,42	46,5	3,7	48	4,47
48,5	3,26	47	3,42	48,5	3,7
49	3,14	47,5	3,25	49	3,43
49,5	3,04	48	3,14	49,5	3,27
50	2,97	48,5	3,04	50	3,16
52	2,76	49	2,97	50,5	3,06
54	2,64	51	2,77	51	2,99
56	2,54	53	2,64	53	2,79
58	2,47	55	2,54	55	2,65
60	2,4	57	2,47	57	2,56
		59	2,41	59	2,49
				61	2,43

Table A-9: Raw Data for Glass Raschig Rings of Titration Method for Set 2.

Glass Packing					
0,1 M NaOH + 0,1 M HCl + 9cm packing					
Liq flow - 122 mL/min		Liq flow - 122 mL/min		Liq flow - 122 mL/min	
16% CO2		12,7% CO2		23,8% CO2	
Run 20		Run 21		Run 19	
Vol(cm3)	pH	Vol(cm3)	pH	Vol(cm3)	pH
0	12,67	0	12,67	0	12,69
5	12,59	5	12,59	5	12,62
10	12,51	10	12,51	10	12,54
15	12,42	15	12,41	15	12,45
20	12,32	20	12,29	20	12,35
22	12,27	22	12,25	22	12,3
24	12,22	24	12,2	24	12,26
26	12,17	26	12,14	26	12,2
28	12,1	28	12,08	28	12,14
30	12,03	30	12	30	12,07
32	11,94	32	11,92	32	11,99
34	11,85	34	11,82	34	11,91
36	11,73	36	11,69	36	11,8
38	11,58	38	11,5	38	11,66
40	11,25	40	11,22	40	11,47
42	10,85	42	10,66	42	11,14
42,5	10,68	42,5	10,44	44	10,51
43	10,48	43	10,22	44,5	10,3

43,5	10,27	43,5	9,95	45	10,08
44	10,03	44	9,53	45,5	9,79
44,5	9,74	44,5	7,96	46	9,38
45	9,29	45	7,17	46,5	7,9
45,5	7,9	45,5	6,77	47	7,35
46	7,38	46	6,39	47,5	7,05
46,5	7,08	46,5	5,91	48	6,76
47	6,76	47	4,36	48,5	6,43
47,5	6,4	47,5	3,65	49	6,06
48	5,99	48	3,4	49,5	4,59
48,5	4,44	48,5	3,25	50	3,71
49	3,66	49	3,14	50,5	3,43
49,5	3,4	49,5	3,05	51	3,27
50	3,24	50	2,98	51,5	3,15
50,5	3,12	52	2,78	52	3,06
51	3,04	54	2,65	52,5	2,99
53	2,8	56	2,54	53	2,93
55	2,66	58	2,48	55	2,75
57	2,57	60	2,42	57	2,64
59	2,48			59	2,55
61	2,42			61	2,47
				63	2,41

Table A-10: Raw Data for Unmodified Raschig Rings of Titration Method for Set 3.

Unmodified Packing					

Unmodified Packing					
0,02 M NaOH + 0,01 M HCl + 28cm packing					
Liq flow - 555 mL/min		Liq flow - 122 mL/min		Liq flow - 390 mL/min	
16% CO2		16% CO2		16% CO2	
Run 22		Run 23		Run 24	
Vol(cm3)	pH	Vol(cm3)	pH	Vol(cm3)	pH
0	11,18	0	11,27	0	11,36
5	11,03	5	11,17	5	11,24
10	10,81	10	11,1	10	11,13
12	10,65	12	11,07	12	11,07
14	10,54	14	11,03	14	11,01
16	10,44	16	10,86	16	10,95
18	10,15	18	10,72	18	10,88
18,5	10,11	20	10,64	20	10,79
19	10,05	22	10,53	22	10,67
19,5	9,99	24	10,42	24	10,54
20	9,88	26	10,26	26	10,37
20,5	9,82	28	10,1	28	10,08
21	9,72	28,5	10,06	30	9,77
21,5	9,57	29	9,99	30,5	9,66
22	9,44	29,5	9,96	31	9,53
22,5	9,23	30	9,92	31,5	9,36

23	8,9	30,5	9,81	32	9,15
23,5	8,12	31	9,74	32,5	8,63
24	7,62	31,5	9,64	33	7,71
24,5	7,37	32	9,53	33,5	7,39
25	7,12	32,5	9,42	34	7,22
25,5	6,92	33	9,29	34,5	7,12
26	6,84	33,5	9,16	35	6,95
26,5	6,76	34	8,93	36	6,71
27	6,65	34,5	8,23	37	6,5
27,5	6,57	35	7,74	38	6,31
28	6,45	35,5	7,52	38,5	6,25
28,5	6,33	36	7,38	39	6,11
29	6,19	36,5	7,21	39,5	5,86
29,5	5,93	37	7,15	40	5,5
30	5,64	37,5	7,09	40,5	4,75
30,5	5	38	7,02	41	4,3
31	4,43	38,5	6,98	41,5	4,1
31,5	4	39	6,91	42	3,96
32	3,88	39,5	6,84	42,5	3,87
32,5	3,74	40	6,75	43	3,79
33	3,67	41	6,55	45	3,58
35	3,49	42	6,46	47	3,44
37	3,37	43	6,36	49	3,35
39	3,29	43,5	6,3	51	3,27
41	3,14	44	6,24	53	3,21

43	3,09	44,5	6,16	55	3,15
45	3,04	45	6,03	60	3,05
50	2,93	45,5	5,98	65	2,97
55	2,88	46	5,64	70	2,91
60	2,84	46,5	4,79	75	2,86
65	2,78	47	4,34	80	2,81
70	2,74	47,5	4,11	90	2,75
80	2,64	48	3,96	100	2,69
90	2,59	48,5	3,86	110	2,65
100	2,55	49	3,79	120	2,62
110	2,52	49,5	3,72		
120	2,49	50	3,65		
		52	3,49		
		54	3,38		
		56	3,3		
		58	3,23		
		60	3,17		
		65	3,06		
		70	2,97		
		75	2,91		
		80	2,86		
		90	2,78		
		100	2,71		
		110	2,66		
		120	2,62		

Table A-11: Raw Data for Glass Raschig Rings of Titration Method for Set 3.

Glass Packing					
0,02 M NaOH + 0,01 M HCl + 28cm packing					
Liq flow - 555 mL/min		Liq flow - 122 mL/min		Liq flow - 390 mL/min	
16% CO2		16% CO2		16% CO2	
Run 26		Run 27		Run 25	
Vol(cm3)	pH	Vol(cm3)	pH	Vol(cm3)	pH
0	11,26	0	11,46	0	11,48
5	11,12	5	11,34	5	11,37
10	10,93	10	11,12	10	11,25
12	10,88	12	11,05	15	11,11
14	10,76	14	10,98	20	10,95
16	10,59	16	10,89	22	10,87
18	10,39	18	10,79	24	10,79
20	10,18	20	10,66	26	10,7
20,5	10,05	22	10,54	28	10,59
21	9,95	24	10,37	30	10,45
21,5	9,85	26	10,17	32	10,28
22	9,74	26,5	10,11	34	10,06
22,5	9,58	27	10,05	34,5	9,96
23	9,36	27,5	9,95	35	9,85
23,5	8,93	28	9,86	35,5	9,74
24	7,66	28,5	9,76	36	9,6

24,5	7,28	29	9,65	36,5	9,36
25	7,13	29,5	9,52	37	9,03
25,5	7	30	9,35	37,5	7,69
26	6,83	30,5	9,03	38	7,3
26,5	6,62	31	7,77	38,5	7,06
27	6,38	31,5	7,44	39	6,77
27,5	6,2	32	7,31	39,5	6,48
28	5,99	32,5	7,17	40	6,17
28,5	5,67	33	7,06	40,5	5,01
29	5,17	33,5	6,94	41	4,72
29,5	4,39	34	6,84	41,5	4,42
30	4,12	35	6,53	42	4,17
30,5	3,95	36	6,11	42,5	4,03
31	3,84	36,5	5,84	43	3,93
32	3,7	37	5,42	43,5	3,85
33	3,59	37,5	4,68	44	3,79
34	3,5	38	4,28	46	3,59
36	3,38	38,5	4,07	48	3,45
38	3,29	39	3,95	50	3,37
40	3,21	39,5	3,86	52	3,3
42	3,15	40	3,67	54	3,24
44	3,1	42	3,51	56	3,18
46	3,06	44	3,4	58	3,14
48	3,02	46	3,31	60	3,11
50	2,99	48	3,25	65	3,02

55	2,92	50	3,19	70	2,95
60	2,86	52	3,14	75	2,9
65	2,81	54	3,1	80	2,85
70	2,77	56	3,06	90	2,78
80	2,7	58	3,03	100	2,72
90	2,65	60	3	110	2,68
100	2,61	65	2,93	120	2,64
110	2,58	70	2,88		
120	2,55	75	2,83		
		80	2,8		
		90	2,74		
		100	2,69		
		110	2,65		
		120	2,61		

Modified Packing					
0,02 M NaOH + 0,01 M HCl + 28cm packing					
Liq flow - 555 mL/min		Liq flow - 122 mL/min		Liq flow - 390 mL/min	
16% CO2		16% CO2		16% CO2	
Run 28		Run 29		Run 30	
Vol(cm3)	pH	Vol(cm3)	pH	Vol(cm3)	pH
0	11,35	0	11,51	0	11,48
5	11,15	5	11,42	5	11,33
10	11,01	10	11,34	10	11,1
12	10,94	15	11,21	12	11
14	10,86	20	11,1	14	10,89
16	10,76	22	11,03	16	10,76
18	10,67	24	10,96	18	10,65
20	10,54	26	10,9	20	10,5
22	10,38	28	10,82	22	10,31
24	10,15	30	10,73	24	10,06
24,5	10,08	32	10,61	24,5	9,95
25	10	34	10,47	25	9,84
25,5	9,89	36	10,3	25,5	9,73
26	9,76	38	10,08	26	9,45
26,5	9,61	38,5	9,98	26,5	9,23
27	9,39	39	9,9	27	8,67
27,5	8,99	39,5	9,81	27,5	7,86
28	7,64	40	9,7	28	7,63

28,5	7,33	40,5	9,56	28,5	7,35
29	7,12	41	9,38	29	7,12
29,5	6,86	41,5	9,12	29,5	6,92
30	6,69	42	7,81	30	9,71
30,5	6,47	42,5	7,35	30,5	6,42
31	6,2	43	7,15	31	6,19
31,5	5,87	43,5	6,95	31,5	5,94
32	5,13	44	6,75	32	5,65
32,5	4,42	44,5	6,49	32,5	5,18
33	4,15	45	6,14	33	4,59
33,5	4	45,5	5,44	33,5	4,27
34	3,89	46	4,76	34	4,1
34,5	3,8	46,5	4,33	34,5	3,96
35	3,71	47	4,11	35	3,87
37	3,54	47,5	3,99	35,5	3,79
39	3,41	48	3,89	36	3,73
41	3,32	50	3,63	38	3,54
43	3,24	52	3,48	40	3,42
45	3,18	54	3,38	42	3,32
50	3,07	56	3,3	44	3,26
55	2,98	58	3,23	46	3,19
60	2,91	60	3,17	48	3,14
65	2,86	65	3,06	50	3,1
70	2,81	70	2,98	55	3,01
80	2,74	75	2,92	60	2,94

90	2,69	80	2,86	65	2,87
100	2,65	90	2,78	70	2,82
110	2,61	100	2,72	80	2,76
120	2,58	110	2,67	90	2,71
		120	2,63	100	2,66
				110	2,62
				120	2,59

Table A-13: Raw Data for Modified Raschig Rings of Titration Method for Set 4.

Modified Packing					
0,02 M NaOH + 0,01 M HCl + 9cm packing					
Liq flow - 555 mL/min		Liq flow - 122 mL/min		Liq flow - 390 mL/min	
16% CO2		16% CO2		16% CO2	
Run 33		Run 31		Run 32	
Vol(cm3)	pH	Vol(cm3)	pH	Vol(cm3)	pH
0	11,27	0	11,51	0	11,32
5	11,16	5	11,41	5	11,22
10	10,98	10	11,28	10	11,1
12	10,91	15	11,24	12	11,04
14	10,84	20	11,19	14	10,98
16	10,76	22	11,14	16	10,92
18	10,66	24	11,07	18	10,85
20	10,55	26	11,02	20	10,77
22	10,41	28	10,96	22	10,68
24	10,26	30	10,91	24	10,59
26	10,03	32	10,85	26	10,46
28	9,64	34	10,78	28	10,32
28,5	9,48	36	10,71	30	10,12
29	9,27	38	10,64	32	9,81
29,5	8,88	40	10,56	32,5	9,72
30	7,54	42	10,45	33	9,57

30,5	7,22	44	10,36	33,5	9,43
31	7	46	10,27	34	9,22
31,5	6,81	48	10,16	34,5	8,93
32	6,63	50	10,07	35	7,93
32,5	6,43	52	9,97	35,5	7,5
33	6,17	54	9,86	36	7,33
33,5	5,8	56	9,73	36,5	7,2
34	5,02	58	9,58	37	7,04
34,5	4,28	58,5	9,48	37,5	6,85
35	4,01	59	9,35	38	6,66
35,5	3,87	59,5	9,21	38,5	6,41
36	3,78	60	9,08	39	6,19
38	3,51	60,5	8,79	39,5	5,88
40	3,37	61	8,12	40	5,28
42	3,28	61,5	7,5	40,5	4,44
45	3,2	62	7,39	41	4,05
50	3,06	62,5	7,29	41,5	3,85
55	2,96	63	7,21	42	3,73
60	2,88	63,5	7,14	42,5	3,65
65	2,82	64	7,09	43	3,59
70	2,77	65	7,04	45	3,39
80	2,69	66	6,99	47	3,26
90	2,63	67	6,96	49	3,17
100	2,58	68	6,93	51	3,1
110	2,54	69	6,9	53	3,04

120	2,51	70	6,87	55	2,99
		71	6,8	60	2,9
		72	6,74	65	2,82
		74	6,57	70	2,76
		76	6,51	75	2,71
		78	6,34	80	2,67
		79	6,17	90	2,6
		79,5	6,09	100	2,55
		80	5,92	110	2,5
		80,5	5,69	120	2,47
		81	5,31		
		81,5	4,88		
		82	4,46		
		82,5	4,19		
		83	4,01		
		83,5	3,91		
		84	3,79		
		84,5	3,69		
		85	3,61		
		85,5	3,54		
		86	3,47		
		87	3,35		
		88	3,28		
		89	3,21		
		90	3,15		

		94	3,11		
		96	3,08		
		98	3		
		100	2,93		
		102	2,88		
		104	2,83		
		106	2,8		
		108	2,77		
		110	2,75		
		115	2,67		
		120	2,6		
		125	2,55		
		130	2,5		
		135	2,46		
		140	2,42		
		150	2,37		
		160	2,32		
		170	2,28		
		180	2,25		
		190	2,22		
		200	2,19		
		200	2,19		

Table A-14: Raw Data for Glass Raschig Rings of Titration Method for Set 4.

Glass Packing					
0,02 M NaOH + 0,01 M HCl + 9cm packing					
Liq flow - 555 mL/min		Liq flow - 122 mL/min		Liq flow - 390 mL/min	
16% CO2		16% CO2		16% CO2	
Run 36		Run 34		Run 35	
Vol(cm3)	pH	Vol(cm3)	pH	Vol(cm3)	pH
0	11,22	0	11,57	0	11,39
5	11,08	5	11,47	5	11,26
10	10,89	10	11,35	10	11,06
12	10,82	12	11,3	12	11
14	10,73	14	11,25	14	10,93
16	10,62	16	11,2	16	10,83
18	10,51	18	11,15	18	10,73
20	10,34	20	11,11	20	10,62
22	10,13	22	11,04	22	10,5
24	9,78	24	10,99	24	10,35
24,5	9,66	26	10,93	26	10,12
25	9,5	28	10,88	28	9,84
25,5	9,32	30	10,8	28,5	9,76
26	9,08	32	10,73	29	9,66
26,5	8	34	10,64	29,5	9,56
27	7,43	36	10,57	30	9,45

27,5	7,3	38	10,48	30,5	9,28
28	7,11	40	10,39	31	9,05
28,5	6,93	42	10,29	31,5	8,58
29	6,78	44	10,2	32	7,77
29,5	6,58	46	10,1	32,5	7,54
30	6,22	48	9,99	33	7,31
30,5	5,93	50	9,87	33,5	7,19
31	5,22	52	9,73	34	7,08
31,5	4,34	54	9,59	34,5	7,01
32	4,01	56	9,41	35	6,9
32,5	3,83	58	9,15	35,5	6,8
33	3,75	59	8,89	36	6,67
35	3,48	60	8,52	37	6,45
37	3,34	60,5	8,14	38	6,09
39	3,23	61	7,62	38,5	5,86
41	3,16	61,5	7,55	39	5,57
43	3,09	62	7,45	39,5	4,93
45	3,04	62,5	7,37	40	4,28
50	2,93	63	7,32	40,5	4,03
55	2,85	63,5	7,28	41	3,88
60	2,79	64	7,22	43	3,56
65	2,74	64,5	7,17	45	3,4
70	2,7	65	7,14	47	3,29
75	2,66	65,5	7,11	49	3,2
80	2,62	66	7,08	51	3,14

90	2,57	67	7,05	53	3,08
100	2,52	68	6,98	55	3,03
110	2,49	69	6,93	60	2,93
120	2,46	71	6,77	65	2,86
		72	6,72	70	2,8
		74	6,54	75	2,75
		76	6,39	80	2,71
		78	6,25	90	2,64
		79	6,19	100	2,59
		80	6,09	110	2,55
		81	6,03	120	2,51
		82	5,95		
		83	5,87		
		84	5,73		
		85	5,6		
		86	5,47		
		86,5	5,2		
		87	5,01		
		87,5	4,79		
		88	4,4		
		88,5	4,11		
		89	3,92		
		89,5	3,8		
		90	3,7		
		90,5	3,62		

		91	3,56		
		93	3,41		
		95	3,35		
		97	3,25		
		99	3,18		
		101	3,11		
		103	3,06		
		105	3,02		
		107	2,97		
		109	2,94		
		111	2,91		
		116	2,84		
		121	2,78		
		126	2,73		
		131	2,69		
		136	2,66		
		140	2,62		
		150	2,57		
		160	2,52		
		170	2,47		
		180	2,43		
		190	2,39		
		200	2,35		

Table A-15: Raw Data for Unmodified Raschig Rings of Titration Method for Set 4.

Unmodifed Packing					
0,02 M NaOH + 0,01 M HCl + 9cm packing					
Liq flow - 555 mL/min		Liq flow - 122 mL/min		Liq flow - 390 mL/min	
16% CO2		16% CO2		16% CO2	
Run 37		Run 38		Run 39	
Vol(cm3)	pH	Vol(cm3)	pH	Vol(cm3)	pH
0	11,1	0	11,55	0	11,26
5	10,92	5	11,45	5	11,11
10	10,72	10	11,32	10	10,84
12	10,6	12	11,28	12	10,73
14	10,48	14	11,23	14	10,63
16	10,35	16	11,18	16	10,5
18	10,1	18	11,13	18	10,35
18,5	10,05	20	11,08	20	10,13
19	9,98	22	11,02	22	9,85
19,5	9,9	24	10,97	22,5	9,77
20	9,82	26	10,91	23	9,63
20,5	9,72	28	10,84	23,5	9,53
21	9,63	30	10,77	24	9,36
21,5	9,52	32	10,7	24,5	9,15
22	9,37	34	10,62	25	8,13

22,5	9,2	36	10,54	25,5	7,65
23	7,67	38	10,45	26	7,43
23,5	7,22	40	10,36	27	7,23
24	7,03	42	10,26	28	7,07
24,5	6,91	44	10,17	29	6,88
25	6,74	46	10,07	30	6,69
25,5	6,61	48	9,96	31	6,41
26	6,47	50	9,84	31,5	6,03
26,5	6,34	52	9,7	32	5,79
27	6,26	54	9,53	32,5	5,27
27,5	6,14	56	9,32	33	4,51
28	6,02	58	9,02	33,5	4,18
28,5	5,86	59	8,68	34	4,01
29	5,39	60	8,18	34,5	3,9
29,5	4,51	60,5	7,77	35	3,81
30	4,09	61	7,56	37	3,55
30,5	3,88	61,5	7,45	39	3,42
31	3,74	62	7,35	41	3,31
33	3,43	62,5	7,27	43	3,23
35	3,29	63	7,2	45	3,16
37	3,16	63,5	7,15	50	3,04
39	3,07	64	7,1	55	2,96
41	3	64,5	7,05	60	2,89
43	2,95	65	7,02	65	2,84
45	2,9	65,5	6,99	70	2,79

50	2,81	66	6,96	80	2,72
55	2,74	67	6,93	90	2,66
60	2,68	68	6,86	100	2,62
65	2,63	69	6,81	110	2,58
70	2,59	71	6,63	120	2,55
80	2,56	72	6,58		
90	2,5	74	6,4		
100	2,46	76	6,25		
110	2,42	78	6,11		
120	2,39	79	6,05		
		80	5,97		
		81	5,88		
		82	5,75		
		83	5,62		
		84	5,48		
		85	5,22		
		86	4,73		
		86,5	4,36		
		87	4,08		
		87,5	3,88		
		88	3,76		
		88,5	3,66		
		89	3,58		
		89,5	3,52		
		90	3,46		

		91	3,37		
		92	3,3		
		93	3,23		
		94	3,17		
		96	3,08		
		98	3,01		
		100	2,94		
		102	2,89		
		104	2,85		
		106	2,8		
		108	2,77		
		110	2,74		
		115	2,67		
		120	2,61		
		125	2,56		
		130	2,52		
		135	2,49		
		140	2,45		
		150	2,4		
		160	2,35		
		170	2,32		
		180	2,29		
		190	2,26		
		200	2,23		

APPENDIX B: SAMPLE CALCULATIONS

RTD

The following calculations were performed using each discrete concentration-time point for each run. The sample calculation below is shown for Run 1 (RTD) of the glass packing at a flow rate of 830 ml/min. The second data point from Table A-1 of conductivity 12.6 µS/cm was converted to a concentration of 0.0000069 g/ml.

The concentration vs. time graph was constructed by plotting the corresponding concentrations at each time interval. An average of the three runs was taken to construct the average concentration vs. time curve.

Using Equation 1, the mean residence time for Run 1 based on the concentration and time data using a 3 second time interval can be calculated as follows:

$$\tau = \frac{\sum_{i=1}^{\infty} C_i t_i \Delta t_i}{\sum_{i=1}^{\infty} C_i \Delta t_i} \tag{B-1}$$

Therefore,

$$C_i \Delta t_i = 0.0000069 \times 3$$

$$= 2.08 \times 10^{-5} \text{ g. s/ml}$$

And

$$C_i t_i \Delta t_i = 2.08 \times 10^{-5} \times 3$$

$$= 6.25 \times 10^{-5} \text{ g. s}^2/\text{ml}$$

Repeating the above calculation for every data point of Run 1 yields:

$$\sum_{i=1}^{\infty} C_i t_i \Delta t_i = 2.65 \times 10^{-1} \text{ g. s}^2/ml$$

$$\sum_{i=1}^{\infty} C_i \Delta t_i = 2.52 \times 10^{-2} \text{ g. s/ml}$$

.

Therefore,

$$\tau = \frac{2.65 \times 10^{-1}}{2.52 \times 10^{-2}} = 10.55 \text{ s}$$

An average of the mean residence times for all three runs was taken to obtain the mean residence time for the type of packing. The mean residence time of glass packing was found to be 12 s.

To construct the exit age distribution curve, the exit age at each time had to be calculated. This was by making use of Equation 2.

$$E(t) = \frac{Ci}{Area} \tag{B-2}$$

Where: $Area = \sum Ci\Delta t = 2.52{\times}10^{-2}$ g. s/ml

$$E(t) = \frac{Ci}{Area} = 2.75 \times 10^{-4}\ s$$

This calculation was performed for each point in each run and the exit age distribution curves were plotted together with an average exit age distribution curve.

Consistency Test

The consistency test was performed to indicate whether some of the tracer was lost to the system.

The area under the average concentration curve was calculated as follows:

$$Area = \sum Ci\Delta t = 2.52{\times}10^{-2}\text{ g. s/ml} \tag{B-3}$$

The mass of tracer injected into the system was assumed to be 1 g as 10 ml of a 1.17 M tracer solution was injected into the system. A volumetric flowrate of 830 ml/min was used.

$$V = 830\ ml/\min{\times}\frac{1}{60} = 13.83\ ml/s$$

$$\therefore \frac{M}{V} = \frac{1\ g}{13.83\ ml/s} = 7.20 \times 10^{-2}\ g. s/ml$$

By comparing the area under the curve with the above value:

$= 0.0252\ /\ 0.072$

$= 0.35$

Therefore only 35% of tracer exits the column.

Titration Method

The sample calculations for the titration method will be performed on run 28 with equations stated in Chapter 3. The volume of HCl used to neutralise the remaining NaOH in the system is found by getting the difference in the inflection points attained from running the data in Appendix A through a Matlab code. The inflection points for run 28 were 28mL and 32mL. The difference is equal to 4mL which is the volume of HCl used. A 0.01M concentration of HCl used in the run.

$$V_{HCl} \times C_{HCl} = n_{HCl} \tag{3.1}$$

$$4 \times 0.01 = 0.04\ mM$$

$$n_{HCl} = n_{NaOH} \qquad (3.2)$$

Therefore the remaining amount of NaOH in the sample used for the titration is 0.04 mM.

$$Moles\ of\ NaOH\ remaining = n_{NaOH} \times \frac{Total\ volume\ of\ solution}{100} \qquad (3.3)$$

$$Moles\ of\ NaOH\ remaining = 0.04 \times \frac{1100}{100}$$

$$Moles\ of\ NaOH\ remaining = 0.44\ mM$$

The next step is calculate the initial amount of NaOH for the run.

$$Initial\ moles\ of\ NaOH = C_{NaOH} \times V_{NaOH} \qquad (3.4)$$

$$Initial\ moles\ of\ NaOH = 0.02 \times 500$$

$$Initial\ moles\ of\ NaOH = 10\ mM$$

The moles of NaOH reacted is calculated next

$$Moles\ of\ NaOH\ reacted = Initial\ moles\ of\ NaOH - Moles\ of\ NaOH\ remaining \qquad (3.5)$$

$$Moles\ of\ NaOH\ reacted = 10 - 0.44$$

$$Moles\ of\ NaOH\ reacted = 9.56\ mM$$

The relationship shown in the balanced chemical equation shown in equation 3.6 is used to calculate the moles of CO_2 absorbed.

$$2NaOH + CO_2 \rightarrow Na_2CO_3 + H_2O \qquad (3.6)$$
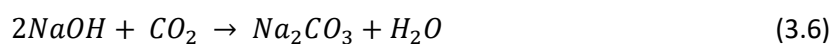
$$Moles\ of\ CO_2\ absorbed = \frac{Moles\ of\ NaOH\ reacted}{2} \qquad (3.7)$$

$$Moles\ of\ CO_2\ absorbed = \frac{9.56}{2}$$

$$Moles\ of\ CO_2\ absorbed = 4.78\ mM$$

The total amount of carbon dioxide absorbed is equal to 4.78 mM and for the results was converted to 2.39 mM/min.

APPENDIX C: CALIBRATION

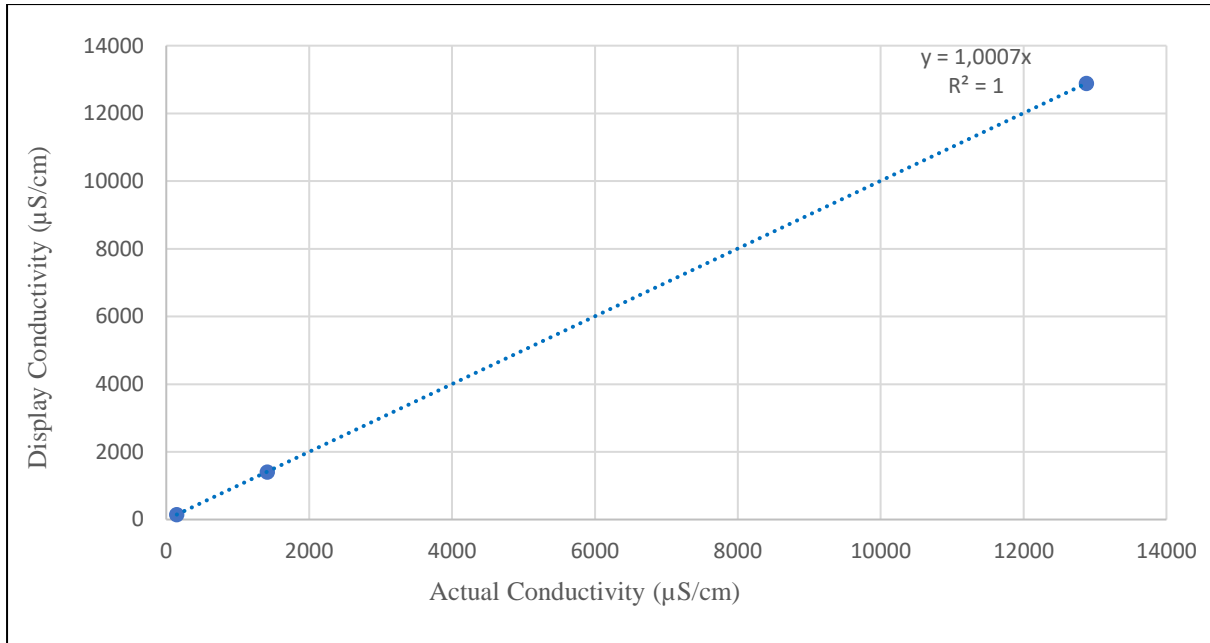## C.1. Part A - Determination of wetting efficiency of polymeric packing

Figure C-1: Calibration Curve Showing the Relationship between Displayed and Actual Conductivity.

Table C-1: Table of Concentration and Conductivity.

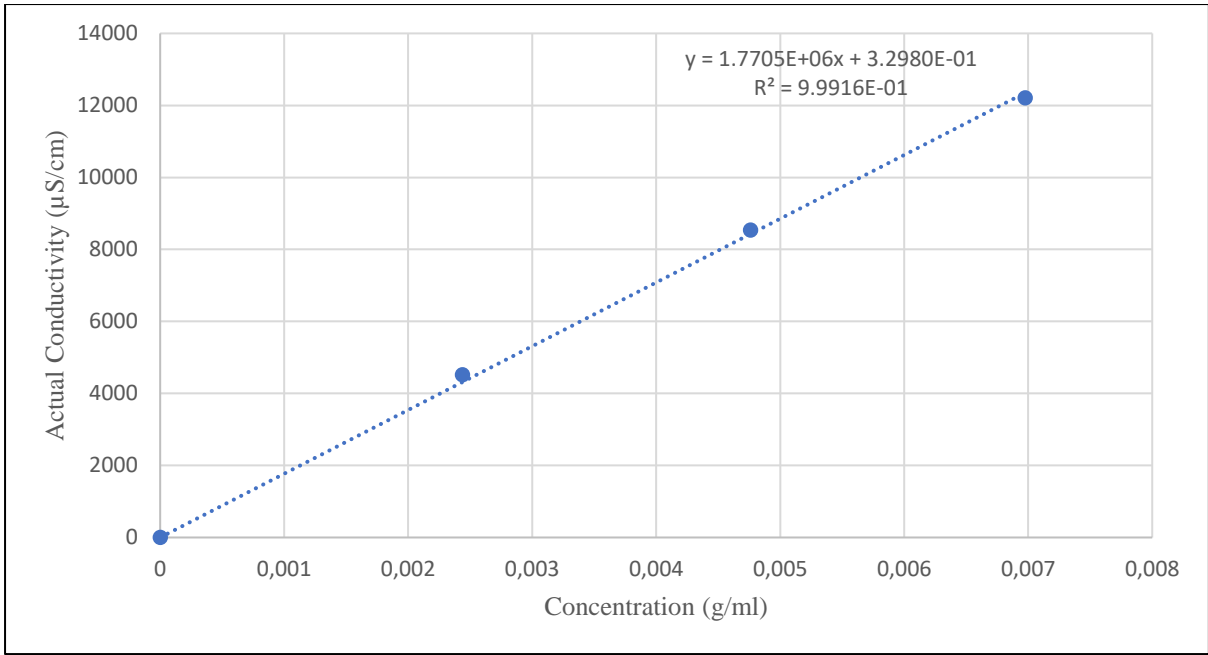| Volume Water (ml)	Aliquot of Salt Solution (ml)	Concentration (g/ml)	Display Conductivity (µS/cm)	Actual Conductivity (µS/cm)
100	0	0	0.33	0.3298
100	2.5	0.00244	4520	4517.2896
100	5	0.00476	8540	8534.8790
100	7.5	0.00698	12220	12212.6724
100	10	0.00909	158000	157905.2568

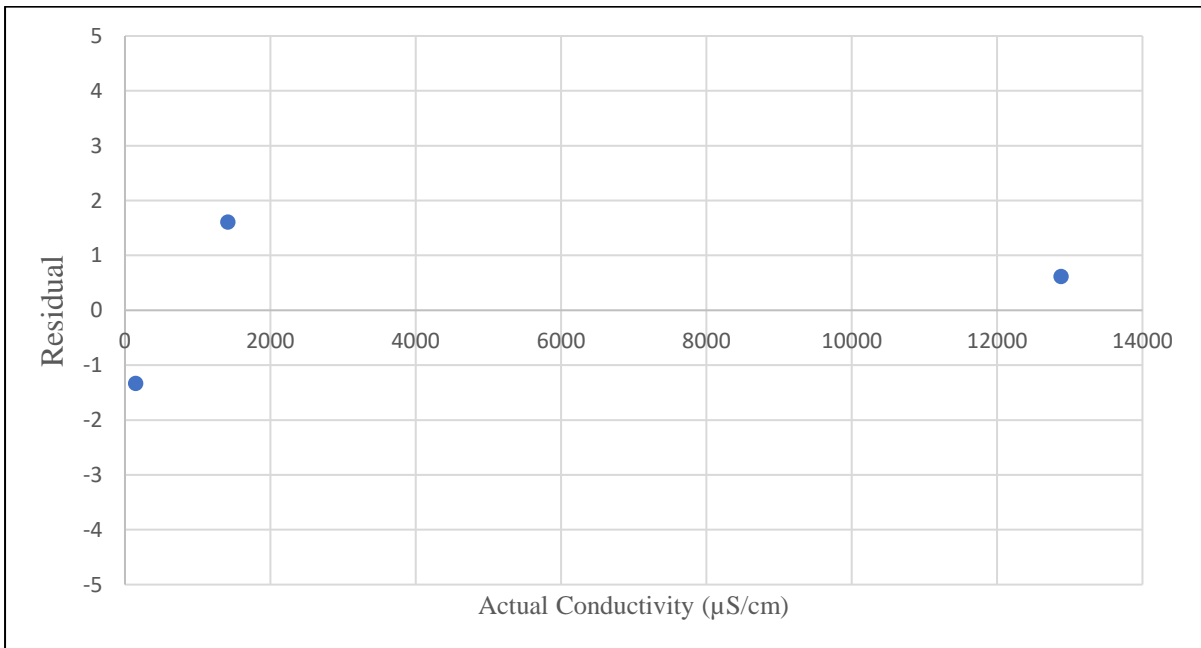*Figure C-2: Graph of Actual Conductivity vs. Concentration.*

Figure C-3: Residual Plot for the Calibration Curve.
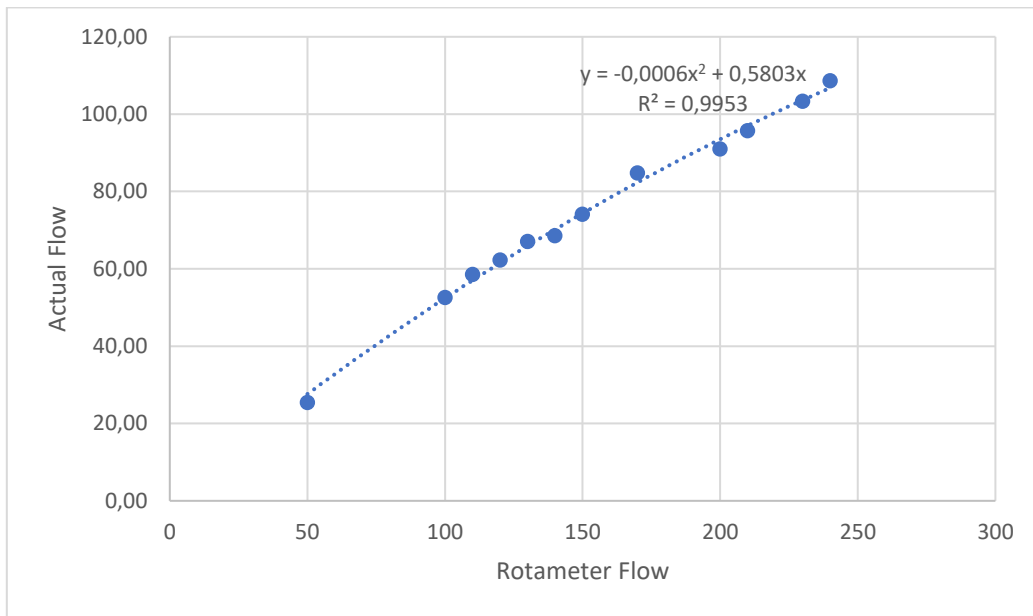
C.2. Part B – Absorption Performance
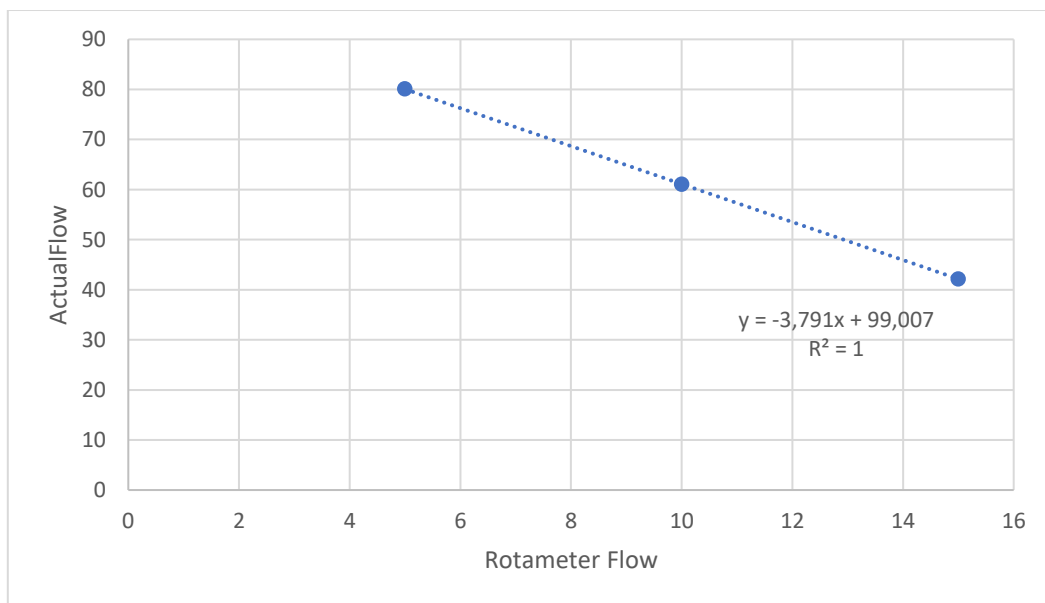

Figure C-4: Nitrogen Rotameter Calibration Curve.

Figure C-5: Carbon Dioxide Rotameter Calibration Curve.